

A STUDY OF THE EFFECT OF VARIOUS FUELS ON
THE OPTIMUM LENGTH OF A GAS TURBINE
COMBUSTOR EQUIPPED WITH A VAPORIZER TUBE

Robert J. Barnes

Thesis
B23

Library
U. S. Naval Postgraduate School
Monterey, California



A STUDY OF THE EFFECT OF VARIOUS FUELS ON THE OPTIMUM
LENGTH OF A GAS TURBINE COMBUSTOR EQUIPPED
WITH A VAPORIZER TUBE

A Thesis
Submitted to the Graduate Faculty
of the
University of Minnesota

by
Robert J. Barnes
LT. U.S. Navy

In partial fulfillment of the
requirements for the degree
of Master of Science in Aeronautical Engineering

Thesis

23

ACKNOWLEDGMENTS

I would like to express my appreciation to the many members of the Mechanical and Aeronautical Engineering Department who assisted in this investigation and in particular, Dr. Newman A. Hall, Professor Thomas E. Murphy, and Mr. Howard M. McManus; and to the Navy group who assisted in the operation of the equipment and reduction of the data.

This project was made possible by the U.S. Navy through the facilities of the U.S. Naval Postgraduate School, Monterey, California.

RJB

May 1954

TABLE OF CONTENTS

	Page
Introduction	1
Experimental Equipment	8
Instrumentation	12
Investigation Procedure	15
Estimated Accuracy of Measurements	22
Discussion of Results	24
Conclusions and Recommendations	32
Appendix	33
Figures	41
Bibliography	63

ILLUSTRATIONS

Figure		Page
1.	Schematic Diagram of Test Cell Apparatus	41
2.	External View of Combustion Chamber	42
3.	Internal View of Combustion Chamber	42
4.	Vaporizer Tube	43
5.	Close-up View of Vaporizer Tube Installed	43
6.	Control Panel	44
7.	Manometer Boards	44
8.	Close-up View of Rake	45
9.	Close-up View of Rake	45
10.	Vaporizer Tube Showing the X, Y, and Z Distances	46
11.	ΔP vs. Mass Flow for Orifice #2	47
11a.	ΔP vs. Mass Flow for Orifice #3	48
12.	Flowmeter Calibration Curves	49
13.	Thermocouple Conversion Chart	50
14.	Typical Air Flow Pattern	51
15.	C_p vs. Temperature for Air	52
16.	Efficiency vs BTU/lb air for Aviation Gasoline	53
17.	Efficiency vs Combustor Length for AvGas	53
18.	Efficiency vs BTU/lb air for Naphtha	54
19.	Efficiency vs Combustor Length for Naphtha	54
20.	Efficiency vs BTU/lb air for Kerosene Fuel	55

Figure	Page
21. Efficiency vs Combustor Length for Kerosene Fuel .	55
22. Efficiency vs BTU/lb air for Diesel Fuel	56
23. Efficiency vs Combustor Length for Diesel Fuel . .	56
24. Efficiency vs BTU/lb air for all Fuels	57
25. Efficiency vs Air-Fuel Ratio for All Fuels	57
26. Efficiency vs Combustor Length for All Fuels . . .	57
27. Flame Pattern for Naphtha, Less Than Design Fuel Flow Rate	58
28. Flame Pattern for Naphtha, Z-Position = 20	59
29. Flame Pattern for Naphtha, Z-Position = 16	59
30. Flame Pattern for Naphtha, Z-Position = 10	59
31. Flame Pattern for Diesel, Z-Position = 10	60
32. Flame Pattern for Kerosene, Z-Position = 10	60
33. Flame Pattern for Aviation Gasoline, Z-Position = 10	61
34. Flame Pattern for Kerosene, Z-Position 20, 16 and 10	61
35. Distillation Curves	61
Appendix A - Computation of the Average Temperature Across Exit Section	33
Appendix B - Computation of Combustion Efficiency	34
Appendix C - Fuel Specifications	38
Table I - Sample Data	35
Table II - ASTM Distillation Data	39
Table III - Fuel Properties	40

Figure	Page
21. Efficiency vs Combustor Length for Kerosene Fuel .	55
22. Efficiency vs BTU/lb air for Diesel Fuel	56
23. Efficiency vs Combustor Length for Diesel Fuel . .	56
24. Efficiency vs BTU/lb air for all Fuels	57
25. Efficiency vs Air-Fuel Ratio for All Fuels	57
26. Efficiency vs Combustor Length for All Fuels . . .	57
27. Flame Pattern for Naphtha, Less Than Design Fuel Flow Rate	58
28. Flame Pattern for Naphtha, Z-Position = 20	59
29. Flame Pattern for Naphtha, Z-Position = 16	59
30. Flame Pattern for Naphtha, Z-Position = 10	59
31. Flame Pattern for Diesel, Z-Position = 10	60
32. Flame Pattern for Kerosene, Z-Position = 10 . . .	60
33. Flame Pattern for Aviation Gasoline, Z-Position = 10	61
34. Flame Pattern for Kerosene, Z-Position 20, 16 and 10	61
35. Distillation Curves	61
Appendix A - Computation of the Average Temperature Across Exit Section	33
Appendix B - Computation of Combustion Efficiency	34
Appendix C - Fuel Specifications	38
Table I - Sample Data	35
Table II - ASTM Distillation Data	39
Table III - Fuel Properties	40

SUMMARY

The need for increasing the speed of the combustion process within a turbojet engine has become of major importance in the jet engine design. One possible means of accomplishing this increase is through the use of a vaporizer tube. Undoubtedly considerable research has been done on this system of fuel injection, but very little information has been published. This investigation was concerned with the effects of various liquid fuels on the combustor length required for maximum efficiency in a given combustion chamber equipped with a vaporizer tube.

Four fuels were tested and it was found that the vaporizer tube produced higher efficiencies than the conventional spray nozzle system. Furthermore, the efficiencies increased with increasing fuel volatility. It was impossible to cool the combustion gases properly with the air flow patterns used in this investigation, therefore, nothing definite can be stated as to the effect of the fuels on the combustor length.

The results obtained, although not final, form a basis for further development in this field.

SYMBOLS

A	- area - square feet
C_p	- specific heat at constant pressure - BTU/lb °F
K	- fuel characteristic factor
M	- mass flow - lbs/sec
P	- pressure - lbs/sq.in. or equivalent
Q	- heat energy - BTU/lb
Q_L	- net heating value of a fuel - BTU/lb
SpGr	- specific gravity at 60°F
T	- temperature - degrees Rankine
t	- temperature - degrees Fahrenheit
H	- total enthalpy - BTU/lb
V	- velocity - ft/sec
η	- combustion efficiency (thermal)
ρ	- density - lbs/cu.ft.
x	- distance from forward end of combustor to point of injection of fuel vapors into chamber - inches
y	- length of return arms of vaporizer tube - inches
z	- position of secondary air pattern
w	- work - BTU/lb

Subscripts

a	- air
abs.	- absolute
act.	- actual

bp	-	boiling point
f	-	fuel
i	-	any recording point in the exhaust cross-section
m	-	mixture
R	-	rake
T	-	total
theo	-	theoretical
1	-	station at orifice #1
2	-	station at orifice #2
3	-	station at orifice #3

INTRODUCTION

Gas turbine engines have reached the stage in development where the degree of reliability and performance is comparable to that of piston engines. Research is now focused on design improvements, new configurations, and methods of increasing the overall efficiency.

One of the greatest problems facing any designer is how to reduce the weight of the engine and at the same time increase the thrust. If any component could be made smaller, a decrease in engine weight through a possible shortening of the whole engine or a decreasing of the overall engine diameter would be possible. A great amount of theoretical analysis has been done on all components of the turbine engine; however, because the process that takes place within a combustion chamber is not completely understood (this is equally applicable to any combustion process), theoretical analysis is hardly possible. Consequently, all present designs of gas turbine combustion chambers are based on experimental data and the trial and error methods.

The most important basic requirements for a satisfactory combustion system are:

- (1) Small size and light weight
- (2) Reliability and easy starting over all ranges of conditions
- (3) Minimum pressure drop

(4) High rate of burning

(5) Complete combustion¹

The combustor must meet the most severe conditions, especially when the combustion intensity is often as high as five times that of a naval boiler. The relatively simple design of all modern combustion chambers has met these requirements so well that a combustor with an overall efficiency of less than 95 per cent at sea level is considered unsatisfactory. Any future improvements naturally will be concerned with the development of better high-temperature metals and a more efficient combustion process. While the former is still being investigated extensively, the combustion process is the subject of much speculation; for the exact nature of any combustion process from the theoretical standpoint is vague.

To understand the important relationship of the combustion process to the present combustor design, a quick look at the air flow pattern is necessary. Basically, all combustors admit air in two parts: the primary air being admitted at the front of the burner to support combustion, and the secondary air being admitted through ports along the burner walls to cool the hot gases of combustion. The amount of secondary air needed is governed by the desired temperature of the exhaust gases that impinge on the turbine blades. To obtain this desired exhaust-temperature profile, a pattern of secondary air (often called quench air) is selected which is desirable and, at the same time, meets other

requirements of the burner. (A pattern is defined as a fixed arrangement of ports relative to one another along the surface of the combustor.) The overall length of the combustion chamber is thus made up of a primary section and a secondary section. The earlier the secondary air can be admitted, the shorter will be the chamber length. Then, once the position of the secondary air pattern is fixed, any further shortening of the burner becomes a problem of shortening the primary section.

It has been shown from the study of combustion processes that raising the inlet temperature of a fuel influences the efficiency and, more important, increases the burning rate of the fuel-air mixture.^{1,2,3} The following brief discussion of the combustion process will stress the importance of these effects on the combustion chamber. In any combustion process a fuel droplet must be vaporized, and must be mixed with the proper amount of air, and must react chemically. These three phases might better be called delay time. This delay time, in turn, consists of two stages, chemical delay (ignition lag) and physical delay time. Chemical delay is that time between the subjection of a fuel to the ignition temperature and the start of combustion. It is thought to be the time required to form the necessary active chain carriers.⁴ Physical delay time is that time required for the fuel to vaporize and mix with the air to form a combustible mixture.

The chemical delay time is a function of the molecular structure and temperature of the fuel. The molecular structure retards the ignition in that its complex structure is broken down into intermediate products before actual combustion begins. The effect of the initial temperature is also important. Preheating a mixture raises the mixture to its flame temperature more quickly. This in turn increases the flame propagation rate, which, for many gases, increases with the square of the absolute temperature. This is particularly important when it is realized that the burning rate dictates the size of a combustion chamber required to burn a given quantity of fuel per unit time.^{5,6,2,3} In gas-turbine combustion chambers a very high burning rate is needed to handle the high combustion intensities.

The physical delay is a combination of fuel characteristics, heat transfer, and mechanical mixing of the air and vapor. A fuel with a relatively high boiling point will require considerable heat transfer before it vaporizes. The proper mixing of vapor and air, which is a very important problem to insure a combustible mixture as soon as possible, is a matter of design.

In an ordinary aircraft-type combustion chamber the fuel is introduced in the form of a spray into the forward end of the chamber where it mixes by turbulence with the primary air, whose sole function is to provide a mixture at or near stoichiometric proportions (later additions of the cooling air will increase the

air-fuel ratio to at least 70 to 1 and higher). Since the fuel and primary air are moving at a finite speed, the length of the primary zone is dependent on the time required to burn the fuel; or, in other words, the length is directly dependent on the delay time and flame speed.

The vaporizer tube, which operates on the principle of a blow-torch, may be an answer to a means of speeding up the combustion process in the primary zone. As the fuel and air pass through the tube, heat from the outside causes the fuel to vaporize and, in some cases of low boiling fuels, to become superheated. The fuel is thus introduced into the primary zone in a gaseous state. Since in an aircraft engine it is not feasible to provide heat for the tube from an external source, the vaporizer tube is located within the primary zone. The exact point of injection of the vaporized fuel into the primary zone is an investigation in itself.⁷ As the fuel leaving the vaporizer tube is more nearly ready for combustion than the fuel from the conventional spray nozzle, the primary zone of the vaporizer type combustor should be shorter than that of the spray type combustor. Pouchot and Hamm found that the outstanding advantage of the vaporizer was a saving of 40 per cent in burner length along with such qualities as high efficiency, stability, usability over large operating ranges, light weight, durability, clean burning, and usability with low fuel pressures.⁸ As Seippel stated, "The greatest step

forward in improving combustion efficiency at high altitudes has been the development of the vaporizer combustion chamber in which fuel lines are passed through a heated section so that the fuel comes out of the nozzle in form of vapor instead of in atomized droplets."⁹

The question arises as to the effect of various fuels of decidedly differing characteristics on the vaporizer tube. Investigations undertaken by the Bureau of Standards revealed that the combustion efficiency of a combustion chamber increased with increasing fuel volatility.⁵ (Efficiency as used here is defined as the actual temperature rise produced by burning a given amount of fuel as compared to the theoretical temperature rise produced by the same amount of fuel.) From the very nature of the vaporizer tube it is reasonable to assume that this volatility effect would be more pronounced within a vaporizer-type combustor. If the tube is exposed to an outside source of heat so that the same amount of heat per unit time passes through the walls of the tube into the fuel, it can be predicted that the lighter fuels will fully vaporize and emerge from the tube at an elevated temperature. On the other hand, the high molecular weight fuels might require so much heat that they would be in a partially liquid state upon leaving the vaporizer tube. Thus, it may be concluded that fuel volatility may be the deciding factor in determining the length of the primary zone.

The purpose of this report is to study the effect of various fuels on the optimum length of a combustor using a vaporizer tube. An open cycle, can-type combustion chamber provided by the Mechanical Engineering Department of the University of Minnesota was modified for this investigation.

EXPERIMENTAL EQUIPMENT

Figure 1 shows a schematic diagram of the test equipment and the associated instrumentation. The equipment has been modified considerably from the original installation designed by Janssen.¹⁰

The air was furnished from two sources. An Allison centrifugal compressor driven by a 165 horsepower, Lycoming, air-cooled, gasoline engine provided the air for the primary and secondary ducts. A high pressure air source furnished the air for the vaporizer tube. This latter source was needed as the Allison compressor was unable to supply the ducts of the chamber and still provide the mass flow through the vaporizer tube.

A stainless steel combustion chamber was used for this investigation. It had a rectangular cross-section, 2" x 5", and was approximately 20" in length (see Figs. 2 and 3). This configuration was originally designed to give two-dimensional flow in the chamber. Air was admitted through 48 ducts spaced at equal intervals around all the chamber except for the exhaust section. Each duct contained a flow straightener, a metering orifice, an injection orifice, and a damper valve for controlling and measuring the air flow. The flow through the vaporizer tube was controlled by a needle valve and measured by a calibrated metering orifice.

There are 39 thermocouples distributed symmetrically

throughout the chamber (see Figures 3 and 5). The thermocouples were connected to a terminal block by the same type of thermocouple wire. Insulated copper wire connected the terminal to the switches on the test cell control panel (see Figure 6). Additional thermocouples were located in the fuel inlet line, in the six-inch intake air duct ahead of the compressor, in the six-inch air duct after the compressor, in the high pressure air line supplying the vaporizer tube, and on the side plate of the combustion chamber.

Two parallel fuel systems were used. The gaseous system consisted of a butane tank as a source from which the gas was supplied to the chamber through a 1/4" copper tubing protruding approximately 1/2 to 3/4 inches into the forward part of the chamber (see Figure 5). The gaseous butane mixture was ignited by a spark plug located about three inches downstream from the gas source. The liquid fuels were pumped through a calibrated flow-meter to the vaporizer tube by a Vickers positive displacement pump. The amount of flow was controlled by a needle valve by-pass system. To insure a sufficient back-pressure, a second needle valve was inserted in the line just prior to the vaporizer tube; and this valve maintained the operating pressure of the fuel line at approximately 15 psig.

The original equipment was modified to allow for the installation of a vaporizer tube in the forward end of the chamber

on the centerline as shown in Figures 3 and 5. The vaporizer tube was made from a $5/8$ " diameter, 20 gage, type 347 stainless steel tubing. The x-distance was maintained at 4" (explained in the next paragraph), and at the beginning of each series of runs the vaporizer tube was checked for possible rotation and misalignment. The scavenging action of the air in the tube carried the fuel into the chamber.

Hereafter in this report the vaporizer tube will be referred to as a cane. This cane that is seen in Figure 4 was selected from a set of various canes investigated in a previous thesis project.⁷ In this project it was established that an x-distance was the optimum point for injecting the gaseous fuel butane into the chamber (see Figure 10). With the x-distance fixed, the y-distance was varied during a series of tests using naphtha. Varying this distance was equivalent to changing the heat transfer area. On the basis of the naphtha tests the 2" cane (so-called because the y-distance equalled 2") was selected as it was felt that the heat transfer area was sufficiently large enough for satisfactory operation with other fuels of higher molecular weight. Because it was the purpose of this report to investigate the effect of various fuels on a given vaporizer tube, the x and y distances were held constant.

The individual temperature and pressure probes were replaced by a rake, consisting of 7 vertically arranged pitot tubes

(see Figures 8 and 9). Attached to each tube, but far enough downstream so as not to affect the flow around the entrance to the tubes, were single shielded thermocouples. The vertical dimension of the exit cross-section was divided into seven equal areas with a pitot and a thermocouple at the center of each area. The tubes and ceramic insulated thermocouple leads were led out through an airfoil-shaped enclosure that was packed solidly with asbestos. The thermocouples were connected to the terminal board in a similar manner as the others in the chamber. The pitot tubes were led to an adjacent manometer board.

The static pressure of the exit was tapped from two orifices, one on either side of the exit cross-section and located one-fourth and three-fourths of the distance down the respective sides.

INSTRUMENTATION

The metering orifices of the air ducts around the combustion chamber were previously connected in blocks to a common manifold on the manometer board. It was found that during the process of setting any one orifice for a given pressure drop, the indicated pressure drops of the other orifices connected to the same manifold were affected. Setting any pattern resulted in laborious and drawn-out processes. To eliminate the interference of one orifice on another, each metering orifice was connected to its own individual U-tube as shown in Figure 7. This is one of the major modifications of the original installation.

The airflow patterns used in this investigation were identical to those used by Ryberg¹² except for slight modifications. This absolute mass flow through each orifice could have been determined from calibration curves by Janssen¹⁰ although it is doubtful if these curves are still accurate because of possible physical alterations to the orifices. As this investigation was concerned more with relative rather than absolute values it was considered sufficient to set a desired pressure drop across each orifice in inches of water regardless of resulting absolute airflow. It was assumed that the airflow through each orifice remained constant for a given pressure drop. The resultant airflow for an airflow pattern would thus remain unchanged during the investigation.

Approximately 97 per cent of the total airflow through the combustor was supplied through metering orifice #2, which contains a 4-inch square edge orifice plate. With the density of the air as a parameter and a given pressure drop across the orifice the mass flow can be determined from the curves of Figure 11. These curves were constructed in accordance with the Power Test Codes.¹¹ In a similar manner the air through orifice #3, containing a 1.1 inch square edge orifice plate, was computed and plotted in Figure 11a. The control of the air flow through orifice #2 was a direct function of the compressor RPM while the small amount through orifice #3 was controlled by a needle valve in the high pressure line.

The liquid fuel flow of the four fuels used in this investigation was measured by a flowmeter which was calibrated for flows from 1.5 to 6.0 gals/hour as indicated on the flowmeter. The calibration curves are shown in Figure 12.

All thermocouples were read by Leeds and Northrup potentiometers. Since the potentiometers were calibrated for iron-constantine thermocouples it was necessary to convert the readings of the chromel-alumel thermocouples. Figure 13 gives this conversion directly to degrees Rankine. The position error of the rake temperature readings because of streamwise displacement of the thermocouples relative to the pitot tube entrances is considered negligible.

The exit section static pressure and pitot readings were

measured on a common manometer board from which the velocity pressure head could be read directly in inches of water.

INVESTIGATION PROCEDURE

For an adequate comparison of the effects of a vaporizer tube with that of a spray nozzle injection system, it was necessary to hold constant as many corresponding variables as possible. The basic conditions of heat release, amount of airflow, and type of airflow patterns were duplicated as given in a previous report by Ryberg.¹² The fuel flow was adjusted to give an available heat release of 93.85 BTU/sec which has been designated as the design point in this report. The primary air-fuel ratio was held at approximately 36 to 1. As previously pointed out, the absolute mass flow through each of the 48 ducts was never computed. Instead, the compressor speed was maintained at 1000 RPM which gave the required total flow of approximately 0.60 - 0.62 lb/sec through orifice #2. The flow through orifice #3 was maintained around 0.022 lb/sec. It was found that the control of a given RPM setting was easier to hold than trying to maintain a given pressure drop across an orifice. The cane flow from orifice #3 was determined from heat transfer computations used in the basic design of the cane.⁷ This flow is relatively insignificant since it only comprises 3% of the total flow of air. The resulting overall air to fuel ratio was approximately 125 to 1 for design conditions.

The x and y distances were held constant (see Figure 10). The z-distance is defined as that distance between the forward

end of the chamber and the first air port through which the secondary air is admitted. As a matter of convenience, this distance has been designated by a z-position number which corresponds to the number of the forwardmost port of the secondary pattern (see Figure 14). The pattern consists of five consecutive air ports which move as a unit. For example, if ports 16 through 20 make up the secondary pattern, the position is designated as z-position 16. If ports 17 through 21 make up the pattern the position is z-position 17, and so on. From Figure 14 it can be seen that the secondary air pattern, moving as a unit, can be shifted along the chamber from z-position 10 to z-position 20. In actual distance from the forward edge of the chamber this would correspond to $z = 6.5$ inches to $z = 14$ inches. The bleed air, shown on the figure, was a very small amount of airflow through unused ducts to prevent possible burning inside the ducts.

The investigation procedure consisted of two parts. First, it was desirable to hold the fuel flow at a design point corresponding to 93.85 BTU/sec while shifting the secondary pattern to determine the best position as reflected by a peak burner efficiency. This position of the secondary pattern will determine an optimum chamber length for each of the four fuels. This series of runs provided a comparison of the effects of fuels with other combustors utilizing different means of fuel injection. Secondly, it was desirable to compare the effects of each fuel through varying the

air-fuel ratio. The secondary air pattern remained fixed at the extreme end of the combustor, and the air flow was held constant while the fuel flow rate was varied. In the first series of runs the results were plotted on a curve of efficiency versus combustor length. In the second series of runs the fuels were compared on the basis of two curves, efficiency versus BTU/lb of air and efficiency versus air-fuel ratio.

The actual mechanics for conducting runs were duplicated as nearly as possible for each run to minimize possible errors in procedure. The term, run, is defined to be the taking of a given set of data with one fuel flow rate, one air pattern, and all equipment stabilized at operating conditions.

The engine and compressor were started and warmed up, allowing at least 10 minutes of operation at normal speed to stabilize the engine and ambient temperatures. The cane air was turned on about 5-10 minutes before commencement of the runs and allowed to flow at design conditions. This was found to be particularly important since the type of compressor providing the high pressure source for the cane air was capable of changing the air temperature and pressures rapidly at the commencement of a series of runs. This time interval allowed the compressor and its high pressure tank supply to stabilize in temperature.

The desired primary and secondary patterns were set accurately. The spark ignition was turned on, and the butane flow

started to provide temperatures in the neighborhood of 800-1000°F around the cane. An excessive combustion intensity was easily obtained with butane and, therefore, it was necessary to observe chamber temperatures closely to avoid burning out thermocouples. After the chamber temperatures were stabilized in the forward section (about one minute elapsed time) the fuel pump was started, and the liquid fuel was introduced into the cane. The liquid fuel flow rate was slow at first until commencement of vaporization and subsequent burning. This was indicated by a noticeable increase in "combustor-roar." The butane flow was slowly shut off, and finally the spark ignition turned off.

Some precautions were needed for the starting of combustion of the heavier fuels, kerosene and diesel. It was necessary to burn the butane torch at a much higher rate for a considerably longer period of time before the cane was hot enough to vaporize the fuel. Then the fuels were introduced at a very slow rate, increasing gradually, while the butane flow rate was very slowly decreased. As a balance of heat release had to be maintained here, many unsuccessful attempts at starting were made before this technique was developed. It was found that with excessive butane flow and a moderate fuel flow rate the whole chamber mixture was too rich and liquid fuel passed through the chamber unvaporized and unburned. At the same time, if the butane flow rate decreased too fast, there was insufficient heat release to complete all vaporization of the

liquid fuel; and, as a consequence, there was a relatively cool flame in the chamber. Again the liquid fuel passed through the chamber unvaporized. If the chamber was already operating on aviation gasoline or naphtha, no problems were encountered when shifting to heavier fuels as the cane was sufficiently hot for continuous operation during the transition.

After the burner had operated a few minutes on the vaporizer tube, the air patterns, airflow, fuel flow, and RPM were checked and adjusted as necessary. Figure 14 shows a typical airflow pattern used in the runs. All readings were read simultaneously. It was found that with the rake installed two operators were sufficient, one operator recording manometer data in the test cell, and the other regulating engine operation and recording rake temperature data at the control panel. However, for a complete set of data which included some 50 thermocouples readings an additional operator was needed at the control panel. All rake readings were recorded once, then rechecked, and the averages used. Total time for one set of readings averaged about 5 minutes. For the air-fuel runs the same procedure was followed after each setting of a new fuel flow rate. For combustor length computations the fuel flow was maintained at design; the secondary air pattern was set at six positions--10, 12, 14, 16, 18, 20 in that or the reverse order--and the above procedure again followed.

Temperature readings were corrected from Figure 13.

Density was computed from perfect gas law; velocities were computed from the following equation:

$$V = \sqrt{\frac{\Delta P}{\rho} (334.9)}$$

where ΔP = inches of water

ρ = density in lb/cu.ft.

The actual average temperature rise of the exit cross-section, ΔT , is obtained as shown in Appendix A. The burner efficiency, η , was computed as follows:

For this combustion process the steady flow energy equation reduces to $H_2 - H_1 = Q_{in}$. (It is assumed that $Q_{out} = 0$, and $W_{in} = W_{out} = 0$)

$$\text{Then } C_P(T_2 - T_1) = Q_{in}$$

$$\text{or } C_P(\Delta T_{\text{theo}}) = Q_{in}$$

which can be rewritten:

$$M_m C_{P_m} (\Delta T_{\text{theo}}) = Q_L \times M_f$$

$$(\Delta T_{\text{theo}}) = \frac{M_f \times Q_L}{M_m \times C_{P_m}}$$

The application of this equation to the method of computing burner efficiency in this investigation introduces a slight error. The reduced energy equation assumes that the temperature, T , is the total temperature whereas the actual temperature measured in the cross-section is a value between the stream and total temperature.

$$\text{Finally } \eta = \frac{\text{actual temperature rise}}{\text{theoretical temperature rise}} = \frac{\Delta T_{\text{act}}}{\Delta T_{\text{theo}}}$$

The same procedure was followed for all runs. A sample reduction of data for a typical run is given in Appendix B. The fuel

specifications used in this investigation are given in Appendix C.

During this investigation the moisture content of the incoming air never exceeded 0.00572 lb-water/lb-air. This affected the efficiency by less than 1%. An additional effect, not yet fully understood, is that of water on the actual combustion process. However, this is beyond the scope of this investigation.

In the equation for computing the burner efficiency the mass flow of the air was determined by direct measurement from metering orifices #2 and #3. The accuracy of the efficiency as obtained in this manner was in doubt because of probable loss of air through leaks in the ducts around the chamber. To minimize this error, an alternative method for computing the mass flow of air was used. The mass flow-rate/unit area equals $\epsilon \rho V$. The exit cross-section area of the plane containing the entrance of the pitot tubes was A_T square feet. Total mass flow of mixture out the exit was $\epsilon \rho V A_1$, where $A_1 = A_T/7 = 0.01116 \text{ ft.}^2$, then $\epsilon \rho V A_1 - M_f = M_{\text{air}}$ where M_f and M_{air} are the respective masses of fuel and air in lb/sec. This new mass of air was used for a new computation of η . All values obtained as a result of using this corrected mass of air are referred to in this report as corrected values. Those obtained by the former method are called uncorrected values. The results of this investigation as shown in Figs. 16 through 26 are based on the corrected values.

ESTIMATED ACCURACY OF MEASUREMENTS

The flowmeter was read to ± 0.025 gals/hour as indicated on the flowmeter. This corresponds to an efficiency error of less than 1% for all fuels.

Manometers were read to ± 0.05 inches of water or mercury. The reading error was considered negligible. Fluctuations of ± 0.10 inches in the rake did not affect the overall efficiency even though the individual stream tube velocities varied as much as ± 5 ft/sec. No calibration of orifices #2 and #3 were made. It was assumed that the accuracy of the mass flow through each orifice was less than 2% as stated in the Power Test Codes.¹¹

Compressor speed was held to ± 5 RPM. In effect this means there was negligible change in airflow during a given run.

The combustion chamber temperatures were measured by unshielded chromel-alumel thermocouples. Considerable error may be involved because of radiation to the colder chamber walls. Since these measurements were used only as an indication of the flame pattern, approximate temperatures were satisfactory.

The temperature of the exhaust gases were measured by single shielded chromel-alumel thermocouples arranged axially to the stream flow. A steady state condition of heat transfer exists. Heat is transferred to the thermocouple junction by convection, radiation, and impact and away from the junction by radiation and conduction.

As the velocities were low enough to give a Mach number less than 0.3, the stream and total temperatures can be considered as equal. At least five diameters of the thermocouple wire were exposed to the gas stream; therefore, losses due to conduction may be considered negligible. The thermocouple is so small so that radiation from the flame may be neglected. This confines the main source of error to the radiation to the walls. An inspection of the profiles of Figs. 30 through 33 indicate that a given thermocouple will be subjected to approximately the same gas temperature for a series of different fuel runs for the same z-position. It is reasonable to expect that any radiation error for a particular thermocouple would be the same for all runs for a given z-position (all other variables remaining constant). On this basis, any relative error will affect the corresponding points on each curve of Figure 26 an equal amount.

The rake thermocouples were checked in boiling water. A maximum deviation from the average reading was 1.5 degrees. Due to method of construction of the rake it was not feasible to check the thermocouples with molten metals at elevated temperatures.

DISCUSSION OF RESULTS

The purpose of this report was to investigate the effects of fuels on the vaporizer-type combustor. A total of 60 runs were conducted and the results are shown in Figs. 16-26.

The first several naphtha runs were conducted to establish curves of efficiency versus BTU/lb of air, and efficiency versus air-fuel ratio, and at the same time to reproduce some of the runs of the previous investigation of the design of the vaporizer tube.⁷ At the starting of the air-fuel runs the burner was operated at the design point until all of the equipment was stabilized, then the fuel was reduced to a low value consistent with continuous burning. In these very high air-fuel ratios the approach to lean blow-out was detected by two means, namely: a visual observation of a shifting flame front, and audible pulsations. An inspection of the flame pattern in the chamber for a typical lean run, shown in Figure 27, does not indicate any abnormal pattern. The results of these runs are plotted on Figure 18 as BTU/lb of air versus efficiency. A considerable scatter of points is noted which necessitated many additional runs.

With the fuel flow set at design the secondary air pattern was shifted from z-position 1 to z-position 10 to determine the optimum combustor length (see Figure 19). Typical flame patterns of this series of runs are shown in Figs. 28-30. There was no

quenching in any of these runs. (Quenching is defined as the cooling of the gases to 1500°F or less before they leave the exit.)

The next series of runs with diesel fuel was conducted in a similar manner to that for naphtha. An attempt to operate at a fuel flow rate higher than the design point was discontinued when liquid fuel seeped out some of the bottom ports and excessive fuel vapors escaped from thermocouple ports on the side plate. Flow was returned to design and the secondary pattern shifted for a series of tests on combustor length. In all of the runs the fuel burned with a bright yellow flame and fuel vapor continued to escape from loose thermocouple and static ports on the side plate. Several attempts were made, without success, to develop a hotter can surface with the use of the butane torch in hopes of eliminating the excessive fuel vapors that were escaping. However, it was finally concluded that the heat transfer surface of the can was insufficient for full vaporization of diesel fuel. The results of the diesel runs are plotted in Figs. 21-23. The decrease in efficiency as the secondary pattern approaches z-position 10, Figure 23, is more probably due to condensation of fuel vapors rather than to a cooling of the combustible mixture below the flame temperature. The flame pattern for z-position 10, shown in Figure 31 appears normal.

The series of kerosene runs presented the most difficulties, both in operation of equipment and in the ability to reproduce results. The escape of vapor as in diesel runs was again noted

except it was excessive, and raw fuel collected in some of the ducts of the bottom row in all runs. Attempts to plug leaks with ceramic cement were not too successful because of vibrations. Seventeen runs were conducted to establish curves and to recheck doubtful points. Figs. 20-21 show these results and Figure 32 gives a flame pattern for z-position 10. This pattern represents one of the better kerosene runs since the fuel burned with a very clean blue (50%) - yellow (50%) color. The indicated quenching is similar to that discussed in the diesel runs.

A final 6 kerosene runs were conducted at a later date after the chamber ducts had been modified for another investigation and restored to the original configuration of this report. It was reasoned that a fuel flow rate corresponding to the peak efficiency point of the air-fuel curve in Figure 20 might eliminate the poor vaporization problem by cutting down the quantity of fuel to the cane. The fuel flow was set at this rate, approximately 75% of design; all other conditions remained the same, and, the secondary pattern was shifted from z-position 10 to z-position 20. It was discovered that the heat transfer was so inadequate that an increase of raw fuel over that of the design runs escaped from some of the bottom ports. The flame patterns for these runs are very significant and those corresponding to z-positions 10, 16, and 20 are superimposed in Figure 34. These patterns clearly show that only the top half of the cane was bathed in flame. A visual inspection of

the flame during the runs indicated that the flame was mostly confined to the upper portion of the chamber. Attempts to shift the flame front down and forward by use of the butane torch were unsuccessful. The only reasonable explanation as to why the flame front stabilized in this position as shown by the patterns is the possibility of physical alterations to the chamber air ports in the forward area. This series of runs does not definitely indicate that this particular cane has insufficient heat transfer for kerosene as the flame front position was abnormal.

The aviation gasoline runs were conducted uneventfully. Pulsating occurred at the very high air-fuel ratios as in the case of the naphtha series. The results are plotted in Figs. 16 and 17. In Figure 17 there is tendency for the efficiency to drop off at z-position 12 but the decrease is hardly great enough to establish this point as the optimum. The flame pattern for z-position 10 (see Figure 33) indicates no quenching.

An inspection of Figs. 30-33 shows a little change in the velocity and temperature profiles at the exit for the four fuels for a given secondary air pattern. In addition it is noted that these profiles have steep velocity and temperature gradients. Even steeper gradients are noted as the secondary air pattern is moved downstream to z-position 20 (see Figs. 28-30). These profiles are typical of those of all runs of this investigation and are very unsuitable for turbine operation. Desirable profiles can be obtained

by proper quenching as was demonstrated in an investigation by Hutches.¹⁶

A compilation of the results of this investigation are plotted in Figs. 24-26. The plot of efficiency versus air-fuel has been added for supplementary information. In all the runs the heat transfer through the cane may be considered constant since the temperatures in the forward section of the chamber around the cane were nearly constant. Thus all variables for the curves of Figure 24 may be considered fixed except for the fuels. The curves then show a trend toward higher peak efficiencies as the volatility increases. This confirms the predictions. Nothing can be stated definitely as to the horizontal position of the peak efficiency points of each fuel. It is expected that the peaks would shift in the direction of increasing air-fuel ratio; but, the naphtha does not conform to the trend. It is suggested that the naphtha curve may be displaced because of a wide scatter of results shown on Figure 18. There are sufficient points to establish peak efficiency level but not an exact horizontal position.

The effects of the fuels on the optimum combustor length is given in Figure 26. There is a trend for the curves to flatten and, in some cases, fall off as the secondary air is moved forward. The overall change in efficiency for each of the fuels is so little and so gradual that it is impossible to determine an optimum length. This lack of an abrupt change in efficiency is undoubtedly due to

the lack of quenching in any of the runs. There was no attempt to produce quenching by variation of the air pattern since Miller showed that quenching with this secondary air pattern was impossible, even with twice the normal pressure drop across the orifices.⁷ With quenching it might be expected that all the curves would flatten very quickly and fall off more rapidly between z-position 15 to z-position 10. This was confirmed by Hutches in his investigation wherein turbulent quenching was used.¹⁶ Thus in Figure 26 there is no indication as to any optimum combustor length for any of the four fuels.

In addition it is observed that the kerosene curve lies below the diesel curve in Figure 26. This is contrary to theory and the results of the air-fuel runs. The flame patterns show that the case is receiving the same amount of heat in both cases. The only logical explanation is poorer burning in the kerosene cases and a possibility of larger amounts of kerosene vapors escaping out the side plate per unit time.

The dotted curve represents the average values of the four corresponding fuel curves of efficiency versus combustor length for a spray type chamber.¹² This average curve is computed on the same basis as the results of this investigation. It is seen that, in general, the vaporizer tube is approximately 20% more efficient than a spray nozzle. This too was previously confirmed in another investigation.⁸

With very few exceptions it was impossible to reproduce a given run within 1% under identical operating conditions. On an average two given runs could be reproduced within 5% with some cases of 10% maximum. The results of the naphtha series of Figure 18 are typical of this scatter. Such a scatter is not unreasonable in combustion investigations; but where two or more curves differ by only a few per cent, a large spread in points could lead to false conclusions.

The efficiencies computed in this report exceeded 100% in a majority of the runs. This is primarily due to the assumption that the temperature and velocity are constant across the face of a stream tube in the horizontal direction. In addition high peak velocities and peak temperatures in the middle of the vertical traverse introduced errors in the integration process of weighting mass flow with the temperatures. These high velocities credit the center portion of the traverse with a larger mass flow than actually exists. This apparent mass flow, in turn, is weighted with excessive temperatures. The result is a further increase in error.

The measuring techniques are difficult in this type of situation. With large temperature gradients the location of the probe is critical as a slight change in probe position results in a large ΔT . Large variations of combustor exit velocity distribution make it difficult regardless of the accuracy of temperature measurements to obtain precise or accurate average temperatures weighted on

the mass flow of gases.¹⁷ In this investigation one or all of the following were evident in each run: wide variation in temperatures, non-uniform velocity distribution, and fluctuations in temperatures. Even with the existence of errors just discussed this particular method of determining the average exit temperature is justified for several reasons: first, this method provides a quick method of reducing data, secondly, the results are relative rather than absolute and the errors will be consistent throughout the reduction process, third, the relative trends and relationships established by the results will provide valuable information.

Some additional observations which could affect the accuracy of the results are listed as follows:

(1) After observing the visual loss of vapor in the kerosene and diesel series, there is some doubt as to whether vapors from all of the fuels did not escape through the side plate.

(2) In the first series of investigations consisting of approximately 75 runs there was a glowing red side plate for nearly all the runs.⁷ In this investigation consisting of 60 runs there were very few (approximately 5-6) runs with a red side plate. Operating conditions were the same in both investigations. This indicates a possible shifting of the flame front although there was physical alteration to the chamber.

(3) In general the efficiency was high with the secondary pattern at z-position 18 and low with the pattern at z-position 16.

CONCLUSIONS AND RECOMMENDATIONS

From the data recorded and the foregoing discussions it is concluded that:

(1) fuels introduced into a combustion chamber by means of a vaporizer tube produce higher combustion efficiencies than if introduced by the conventional system,

(2) efficiency increases with increasing fuel volatility,

(3) lack of proper quenching of the hot combustion gases makes it impossible to establish an optimum combustor length for the various fuels,

(4) performance with this vaporizer tube was unsatisfactory for kerosene and diesel fuel.

Suggestions for future investigations are submitted as follows:

(1) more basic studies should be devoted to the design of a vaporizer tube to handle heavier fuels,

(2) this combustion chamber operated at an inlet pressure approximating 40,000 feet altitude but at a different inlet temperature from this altitude. In addition, it was an impossibility to control the air leaks from the ducts or the heat loss from the side plates. It is suggested that a combustor be designed that would correct these defects as well as provide a positive control over the inlet and exit temperatures and pressures for wide ranges of operation.

APPENDIX A

COMPUTATION OF THE AVERAGE TEMPERATURE
ACROSS THE EXIT SECTION

The average temperature rise of the exit cross-section was obtained by weighting each of the seven rake temperature readings with a respective stream tube mass flow. The vertical dimension of the exit cross-section was divided into seven equal parts, forming seven stream tubes of equal cross-sectional area. At the center of each stream tube a temperature and total pressure were recorded. From this temperature and the exit static pressure a density was computed for each stream tube. The velocity of each stream tube was computed from the density and a ΔP (total pressure minus exit static pressure).

If ρ_i = density for each stream tube

V_i = velocity for each stream tube

T_i = temperature for each stream tube

T_{ave} = mass flow weighted temperature rise across the exit section in degrees Rankine

A_i = area of the cross-section of each stream tube

$\sum \rho_i V_i A_i$ = mass flow rate through exit

$$\text{then } T_{ave} = \frac{\sum (\rho_i V_i A_i) T_i}{\sum (\rho_i V_i A_i)} = \frac{\sum \rho_i V_i T_i}{\sum \rho_i V_i}$$

APPENDIX B

COMPUTATION OF COMBUSTION EFFICIENCY

The recorded data obtained from each run was the following:

P_a	atmospheric - inches of mercury
T_a	atmospheric temperature ahead of compressor - $^{\circ}\text{R}$
T_2	air temperature after compressor - $^{\circ}\text{R}$
T_3	cane air temperature - $^{\circ}\text{R}$
T_1	profile temperature of exhaust cross-section (consisted of seven readings) - $^{\circ}\text{R}$
P_R	static pressure in exhaust section at rake - inches of water
P_2	static pressure at orifice #2 - inches of water
P_3	static pressure of cane air - inches of mercury
Z	position of the secondary air pattern

To find the combustion efficiency it was necessary to compute the following quantities:

ρ_1	density of each stream tube of the exit area - lb/cu.ft
V_1	velocity of each stream tube - ft/sec
$(\rho V)_1$	momentum flow per unit area through exit - lb/ft ² -sec
$(\rho VT)_1$	mass weighted momentum temperature flow through the exit - lb/ft ² -sec- $^{\circ}\text{R}$
T_{ave}	actual average temperature of the exit cross-section - $^{\circ}\text{R}$
c_{Pair}	read from curve of Figure 15 - BTU/lb - $^{\circ}\text{R}$
c_{pm}	specific heat of the mixture - BTU/lb- $^{\circ}\text{R}$
$M_f \times Q_L$	heat available from the fuel - BTU/sec

M_T total mass flow through exit area - lb/sec = $\sum (\rho V)_i A_i$

M_a total mass flow of air - lb/sec = $\sum (\rho V)_i A_i - M_f$

The following table gives the sample data taken from a typical run of aviation gas:

TABLE I
SAMPLE DATA

1	2	3	4	5	6	7	8
T_{-OR}	P_R "water	P "H ₂ O	$(P_R)_{abs}$ "Hg	P lb/ft ³	V fps	ρV	ρVT
652	(-)2.90	0.60	28.86	.0582	59	3.3435	2239
715	"	4.55	"	.0534	169	9.025	6455
1039	"	8.50	"	.0367	277	10.165	10560
1957	"	9.80	"	.0193	410	7.915	15480
1820	"	9.15	"	.0208	384	7.99	15450
888	"	6.25	"	.0385	233	8.975	8865
698	"	2.15	"	.0544	115	<u>6.26</u>	<u>4368</u>
						53.76	62507

Col. 1 - seven rake temperature readings

Col. 2 - static pressure at exit

Col. 3 - P for 7 rake positions

Columns 1,2,3 are recorded during the run and in addition

$P_a = 29.07$ inches of mercury

$P_R = (-) 2.90$ inches of water = $(-) 0.21$ inches mercury

$T_2 = 553$ °R

$T_3 = 533$ °R

Column 4 - the absolute static pressure of each stream tube

Column 5 - computed from the perfect gas law, using cols. 1 and 4

Column 6 - computed from cols. 3 and 5

Column 7 - product of cols. 5 and 6

Column 8 - product of cols. 1,5, and 6

$$T_{ave} = \frac{(\rho VT)_1}{(\rho V)_1} = \frac{62507}{53.76} = 1163 \text{ } ^\circ\text{R}$$

The combination of temperatures T_2 and T_3 weighted with their respective mass air flow gives a temperature of the air entering the chamber through the ducts as one degree less than T_2 .

Therefore $\Delta T_{actual} = 1163 - 552 = 611 \text{ } ^\circ\text{R}$ (temp. rise through combustion chamber)

$$M_T = (\rho V)_1 A = 53.76 \times .01116 = .6000 \text{ lb/sec}$$

$$M_a = .6000 - .004654 = .5954 \text{ lb/sec}$$

$$C_{p_{air}} = .2462 \text{ (from Figure 15)}^{18}$$

$$M_a C_{p_a} = .2462 \times .5954 = .1460$$

$$M_f c_{p_f} = .004654 \times .520 = .0025$$

$$C_{p_m} = \frac{M_f \times C_{p_f} + M_a \times C_{p_a}}{M_m} = \frac{.0025 + .1460}{.6000} = .2475$$

$$\Delta T_{theo} = \frac{M_f \times Q_L}{M_m \times C_{p_m}} = \frac{.004654 \times 18726}{.6000 \times .2475} = 586 \text{ } ^\circ\text{R}$$

$$\eta = \frac{(\Delta T)_{actual}}{(\Delta T)_{theo}} = \frac{611}{586} = 104.2\%$$

$$\text{BTU/lb-air} = \frac{.004654 \times 18726}{.5954} = 146.5$$

$$\text{Ratio of Air/fuel} = \frac{.5954}{.004654} = 128$$

The uncorrected values of η , BTU/lb-air, and air-fuel ratio are computed in a similar manner only the value, M_a , is determined from the summation of the mass flow through the orifices #2 and #3. For example:

at orifice #2: $P_T = 30.69$ inches of mercury

$$\Delta P = 4.00 \text{ inches of water}$$

$$\rho = .0740 \text{ lb/ft}^3$$

$$M_a = .5870 \text{ (from Figure 11)}$$

at orifice #3 $P_T = 32.91$ inches of mercury

$$\Delta P = 1.42 \text{ inches of water}$$

$$\rho = .0817 \text{ lb/ft}^3$$

$$M_a = .0219 \text{ (from Figure 11)}$$

Total mass flow through chamber = $.5870 + .0219 = .6089 \text{ lb/sec.}$

Based on this value, $\eta = 107\%$

$$\text{BTU/lb-air} = 143$$

$$\text{Ratio of Air/fuel} = 131$$

APPENDIX C

FUEL SPECIFICATIONS

The four fuels used in this investigation are the same as those used in the report by Ryberg.¹² Although the values of the specific gravity of a particular fuel as used in each investigation differed somewhat, the overall heating values and specific heats did not vary enough to introduce errors for purposes of comparison.

The heating value, latent heat of vaporization, and the weight per cent of hydrogen and carbon were computed from an equation using the specific gravity.¹³ As these values did not vary appreciably from the various handbook values, they were accepted as being sufficiently accurate for purposes of calculations in this investigation. The equations used are:

$$(1) \text{ net heating value in BTU/lb} = 19960 - [3,780 \times (\text{spgr})^2] - [1362 \times (\text{spgr})] \quad \text{(for const. press.)}$$

$$(2) \text{ latent heat of vaporization in BTU/lb} =$$

$$\frac{110.9 - 0.09 \times \text{temp } ^\circ\text{F}}{\text{sp gr}}$$

where $t^\circ\text{F}$ was chosen as an average between the boiling point and the temp. of the incoming air.

$$(3) \text{ weight } \% \text{ of Hydrogen} = 26 - (15 \times \text{spgr})$$

$$(4) \text{ weight } \% \text{ of carbon} = 100 - \text{wt. } \% \text{ of hydrogen}$$

The specific heats of the fuels were based on equations wherein a factor K was used.² This factor is a direct indication of the fuel characteristics as shown by the equation $K = \frac{\sqrt[3]{T_{bp}}}{\text{spgr @ } 60^\circ\text{F}}$.

It is plotted as a parameter in curves of temperature versus c_p .

From the equation

$$C_{p_{ave}} = 1/6(c_{pt_1} + 4c_{pt_{av}} + c_{pt_2})$$

the average C_p may be calculated. The upper and lower values of the temperatures of the fuel vapor were taken as 800 °F and 1500 °F.

($C_{pt_{av}} = C_p$ from curve at $\frac{t_1 + t_2}{2}$, while $C_{p_{ave}} = \text{final } C_{p_{fuel}}$)

The distillation curves shown in Figure 35 were determined according to the specification given by the ASTM Distillation Code.¹⁴

The vapor pressure of the fuels were determined with a Reid vapor pressure bomb in accordance with the ASTM specifications and standards.¹⁵

Densities were determined by use of the Westphal balance.

Table II lists the distillation data while the fuel properties are found in Table III.

TABLE II
ASTM DISTILLATION DATA

Fuel ml	Aviation Gas °F	Naphtha °F	Kerosene °F	Diesel °F
0	125	229	333	320
5	155	235	370	394
10	163	238	382	417
50	198	252	421	495
90	256	271	479	591
92	266	273	482	598
95	303	278	496	610
Residual	1.2	0.5	1.2	2.0
Loss	1.0	1.3	0.3	2.0

TABLE III

FUEL PROPERTIES

Fuel	Aviation Gas	VM&P* Naphtha	Kerosene	Diesel Fuel #2
Specific gravity @ 60°F	0.7249	0.7624	0.8272	0.8708
API specific grav. @ 60°F	63.7	53.3	39.5	31.0
Pounds of fuel per gal.	6.032	6.374	6.890	7.251
Reid vapor pressure - psig	6.15	0.62	0.32	0.35
Boiling point from dist. curve - °F	204	254	430	495
Latent heat of vapor(const.press.) - BTU/lb	136	126	108	97
Net heating value - BTU/lb	18862	18800	18505	18290
Wt % hydrogen	15.13	15.15	13.6	12.92
Wt % of carbon	84.87	84.85	86.4	87.08
Specific heat - BTU/lb-°F	0.520	0.498	0.519	0.607

*Varnish Makers and Painters' Naphtha

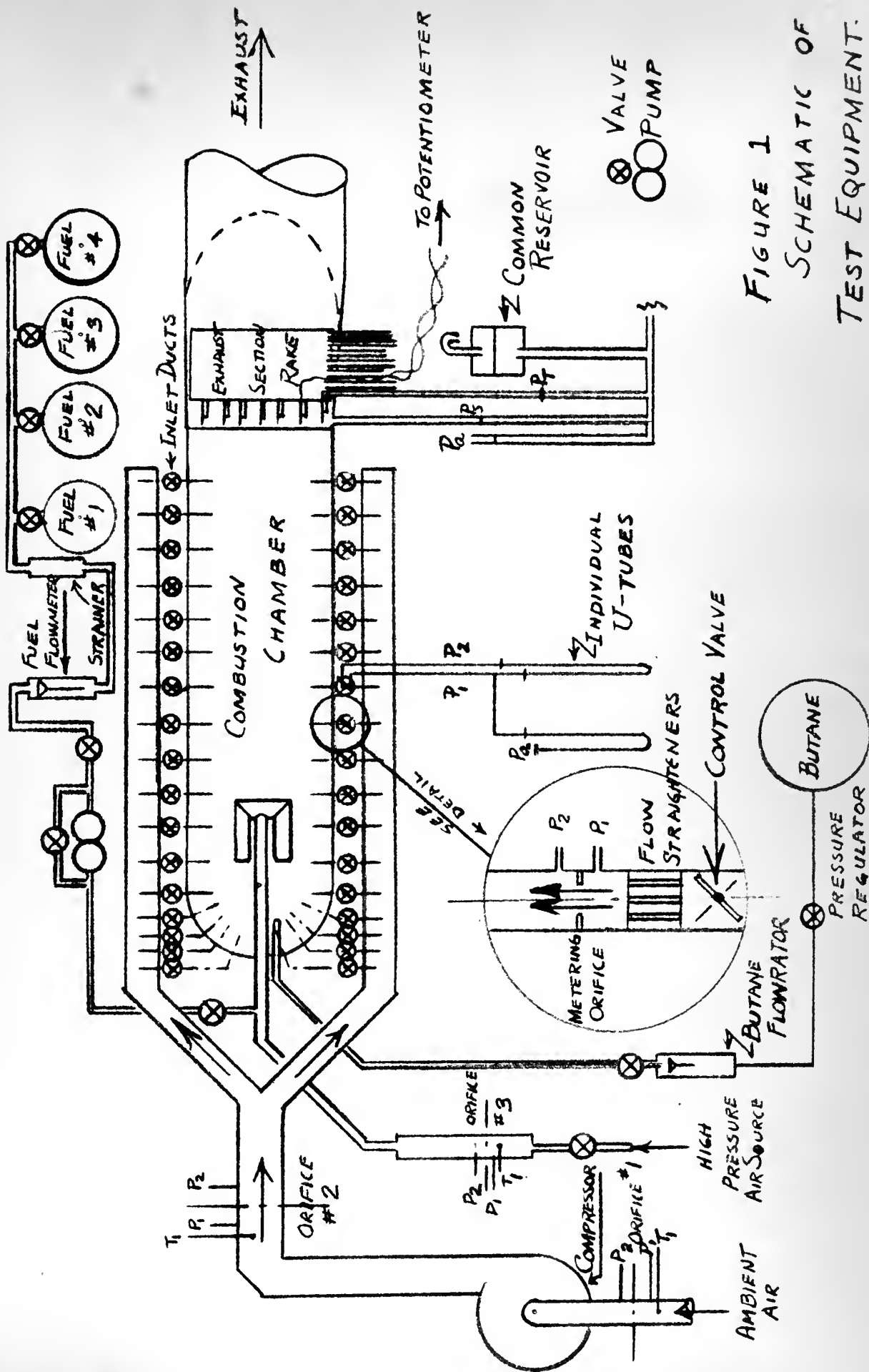


FIGURE 1
SCHEMATIC OF
TEST EQUIPMENT.

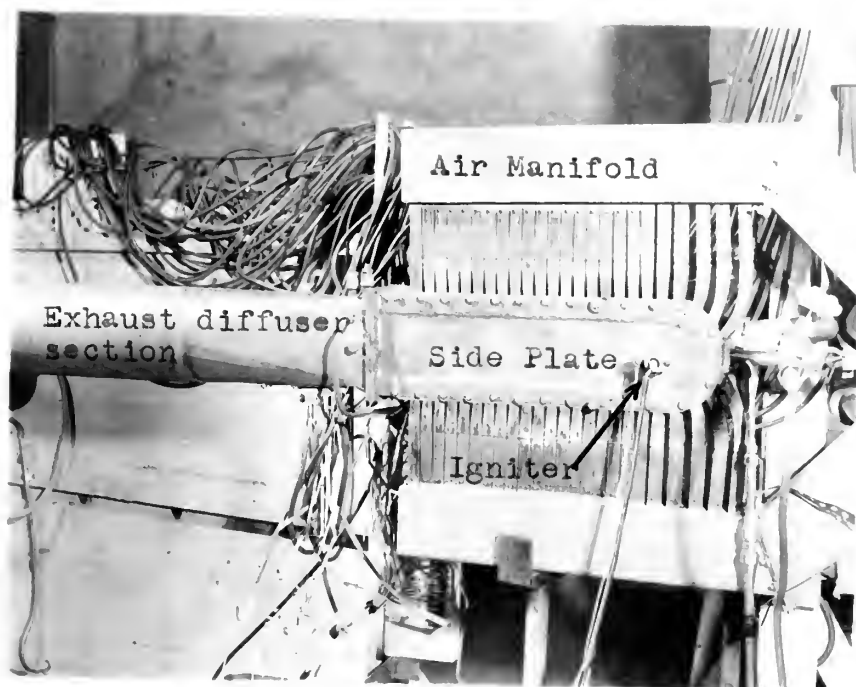


Figure 2. External View of Combustion Chamber

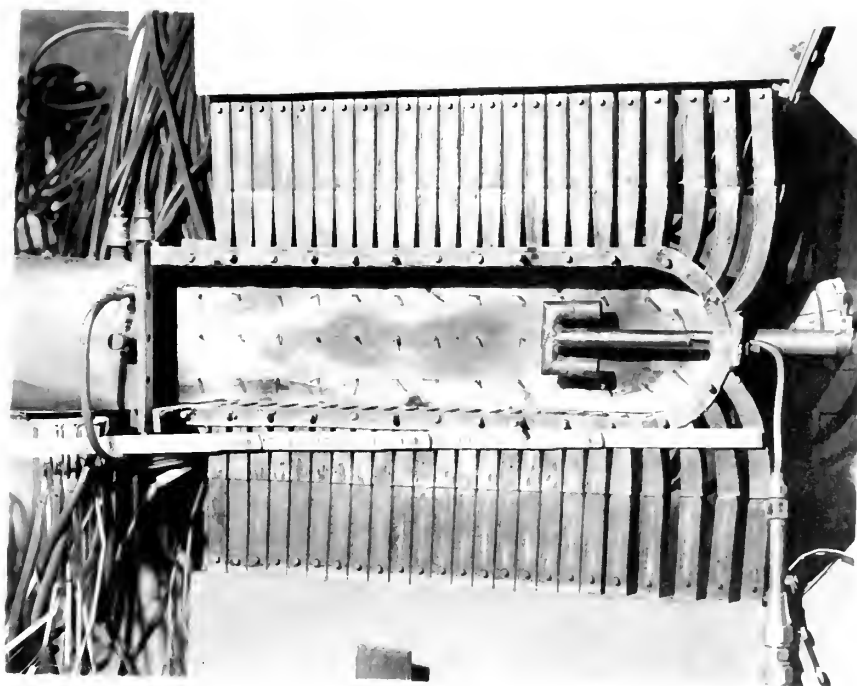


Figure 3. Internal View of Combustion Chamber



Figure 4. Vaporizer Tube

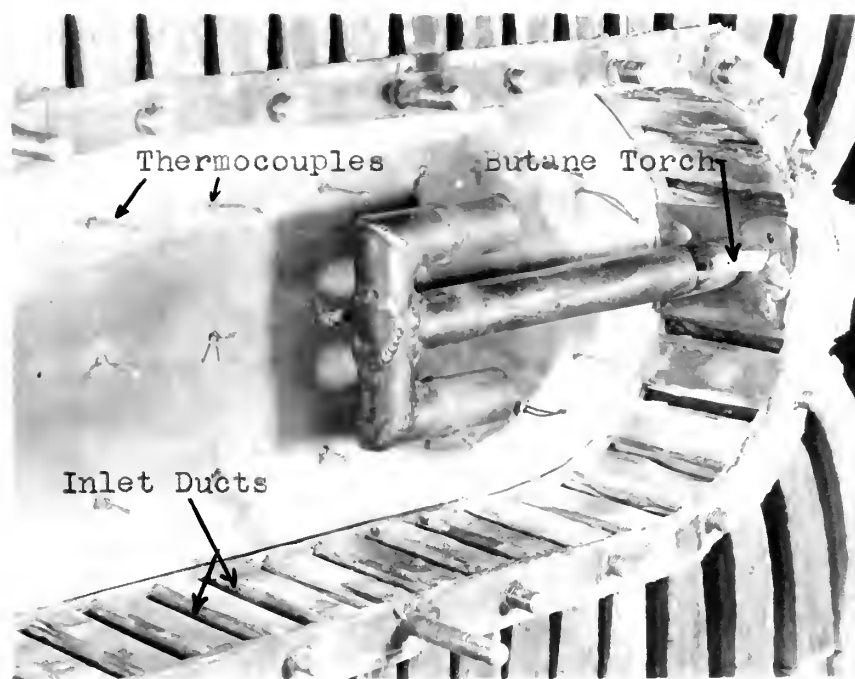


Figure 5. Close-up View of Vaporizer Tube Installed

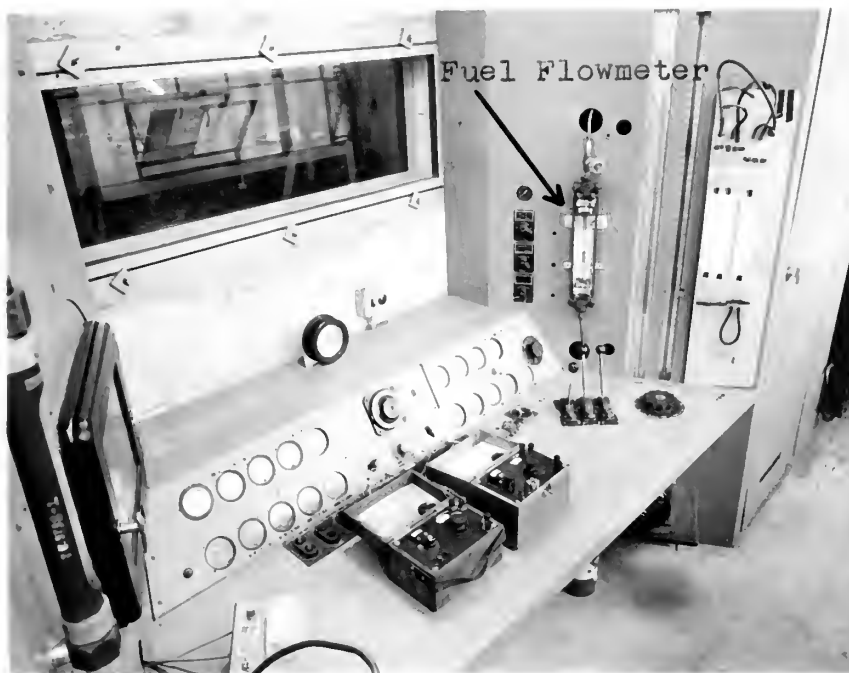


Figure 6. Control Panel



Figure 7. Manometer Boards



Figure 8. Close-up View of Rake

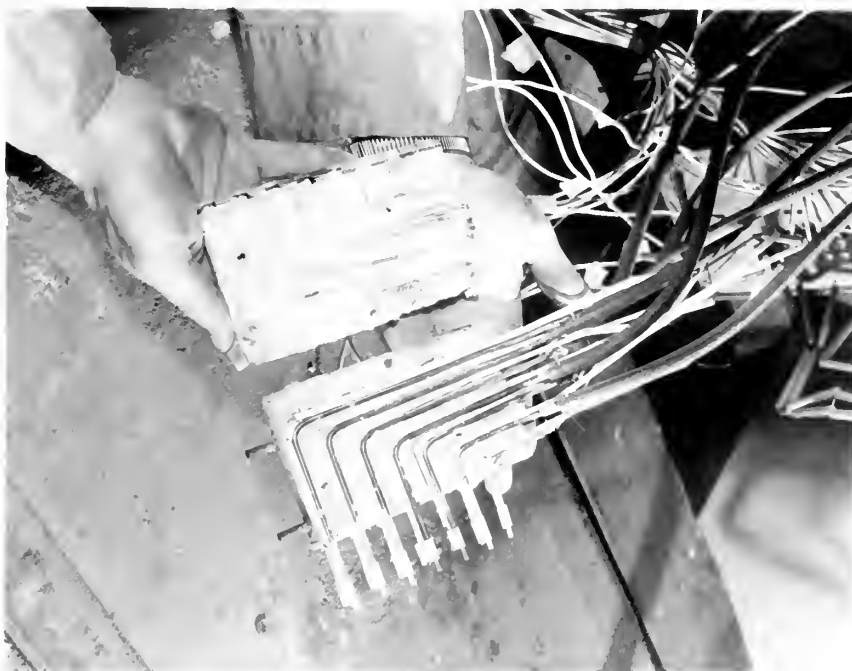


Figure 9. Close-up View of Rake

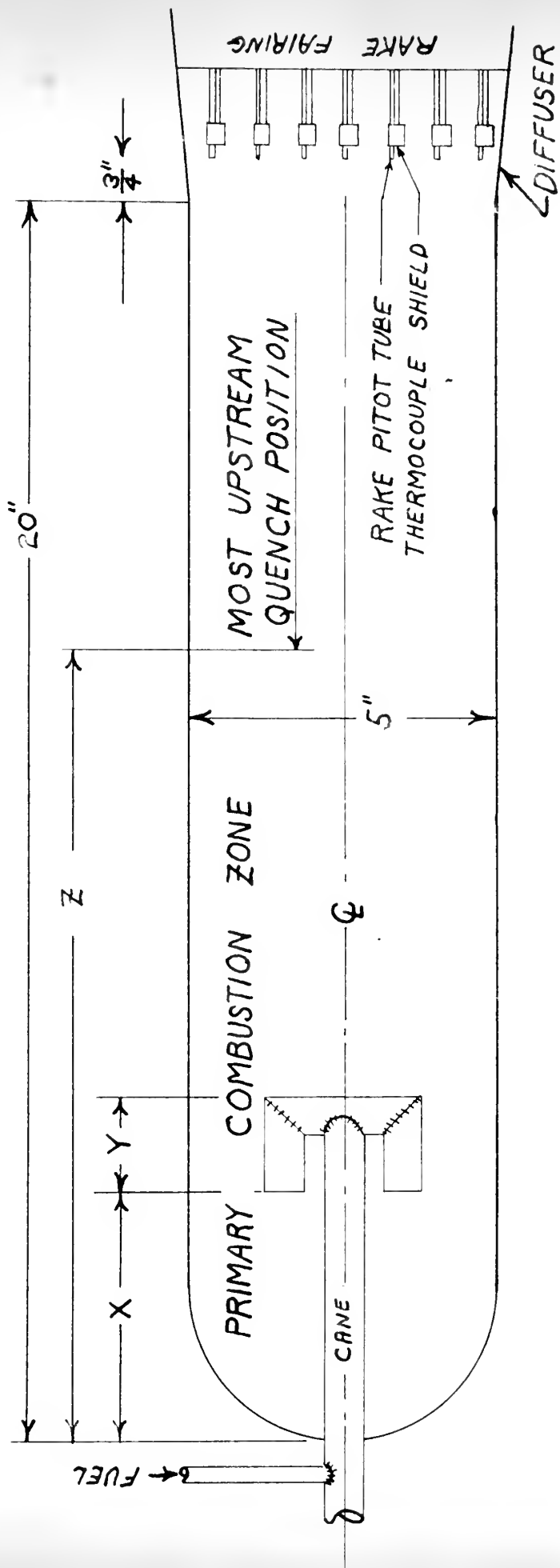


FIG. 10 SIDE ELEVATION OF COMBUSTOR
SHOWING CANE AND RAKE LOCATIONS

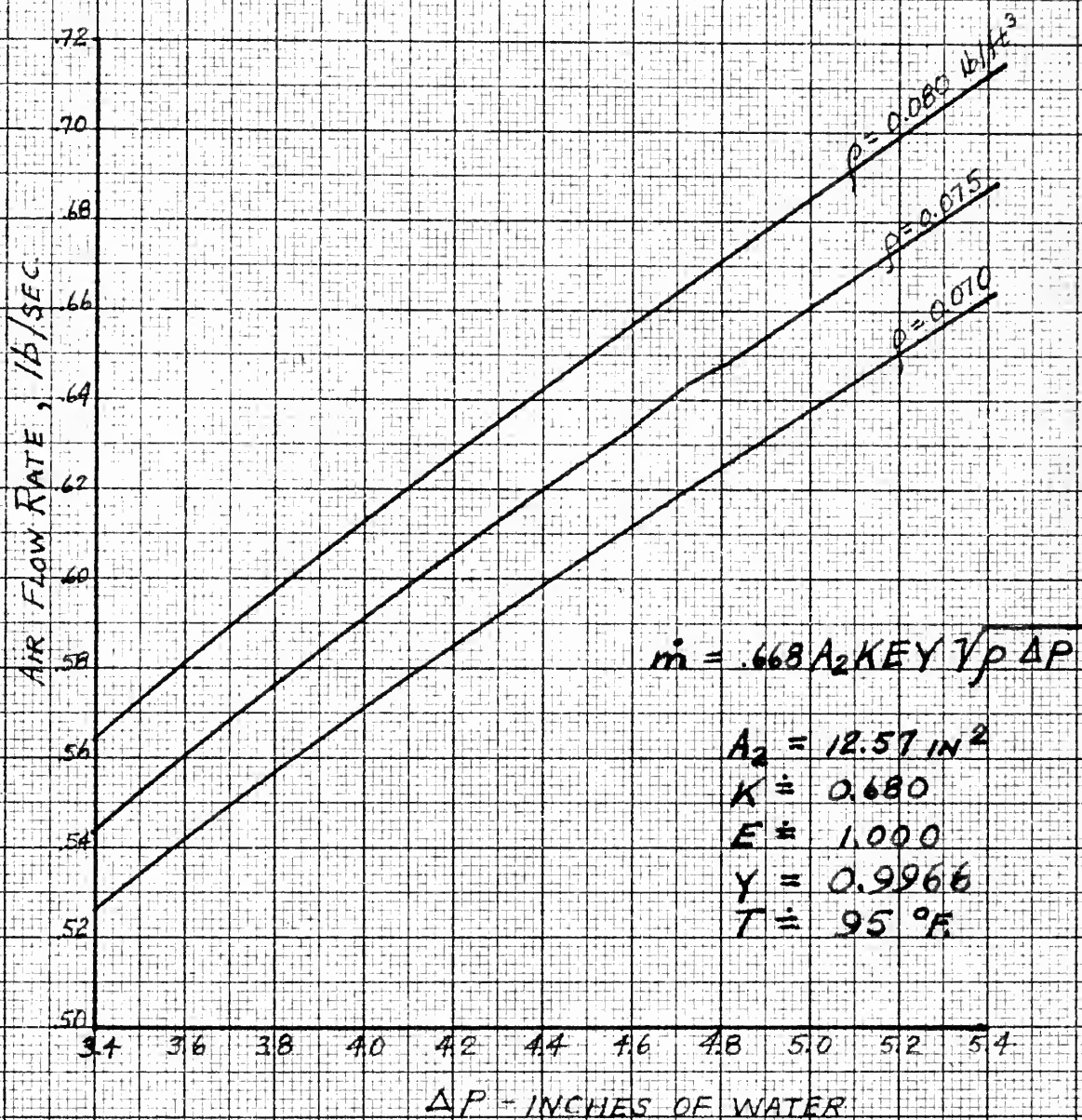


FIGURE 11 - AIR FLOW RATE FOR ORIFICE #2

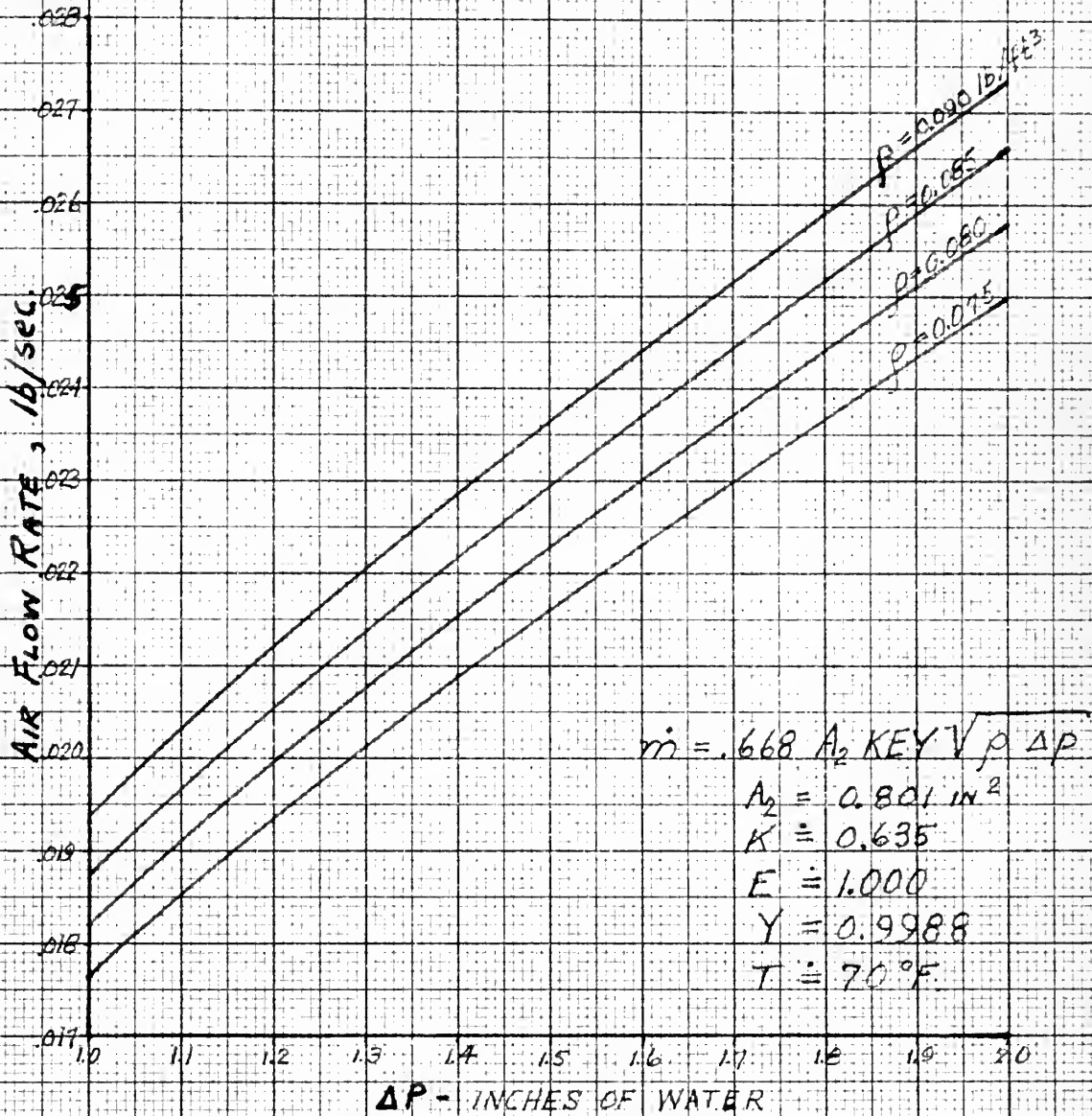


FIGURE 11a - AIR FLOW RATE FOR ORIFICE # 3

Flowmeter - GPH

5.0

4.5

4.0

3.5

3.0

2.5

2.0

1.5

Diesel

Kerosene

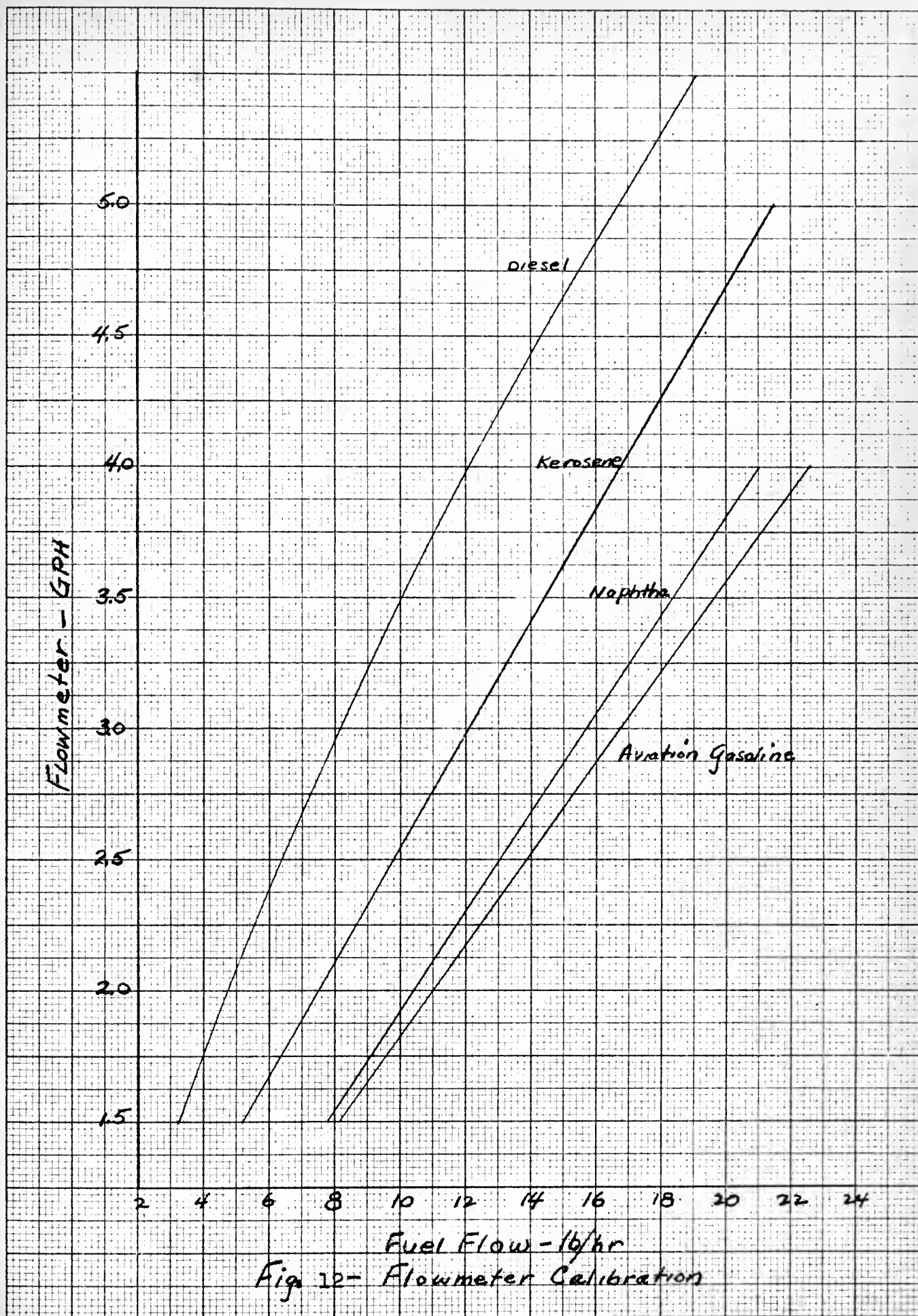
Naphtha

Aviation Gasoline

2 4 6 8 10 12 14 16 18 20 22 24

Fuel Flow - lb/hr

Fig 12- Flowmeter Calibration



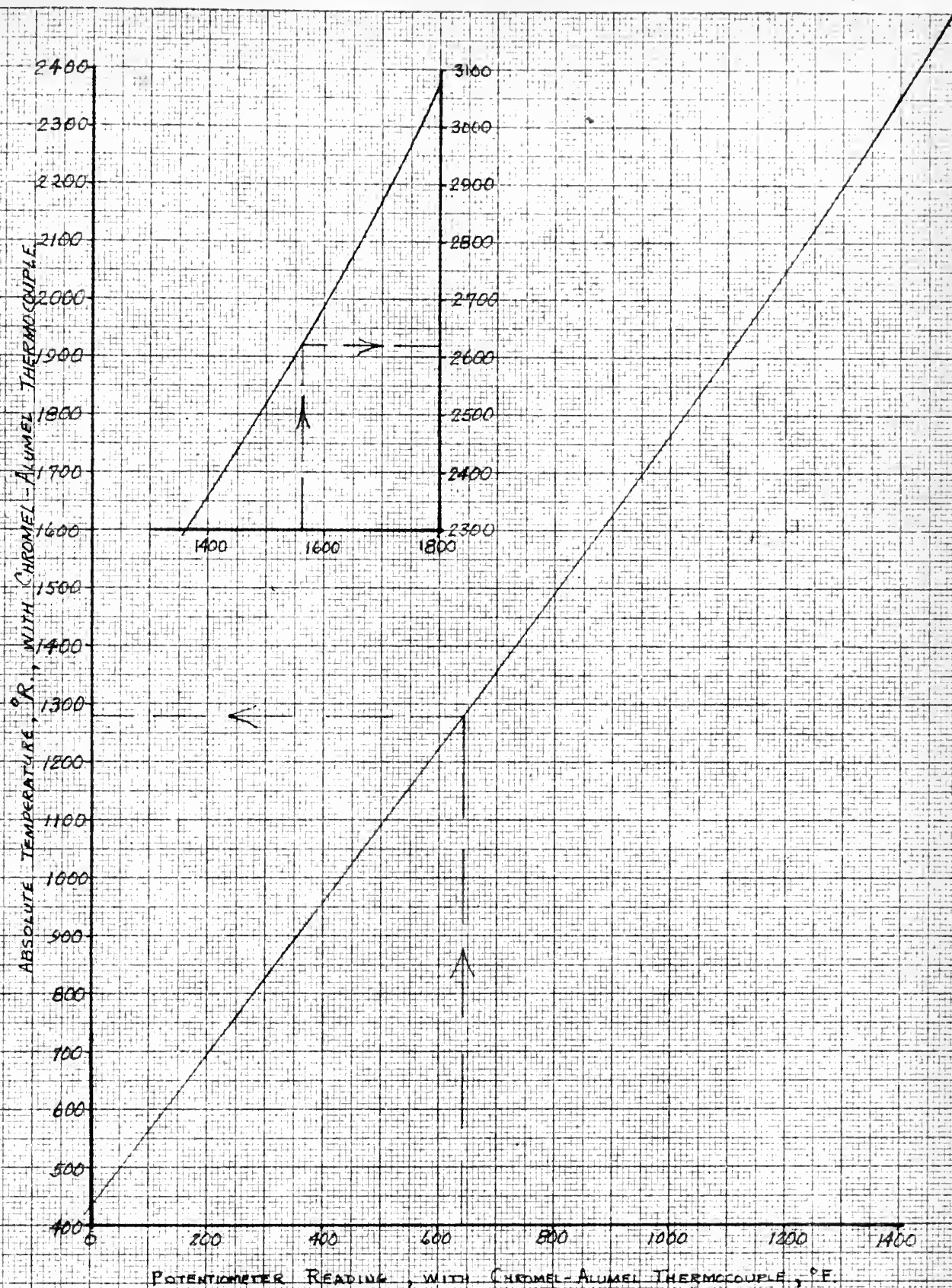
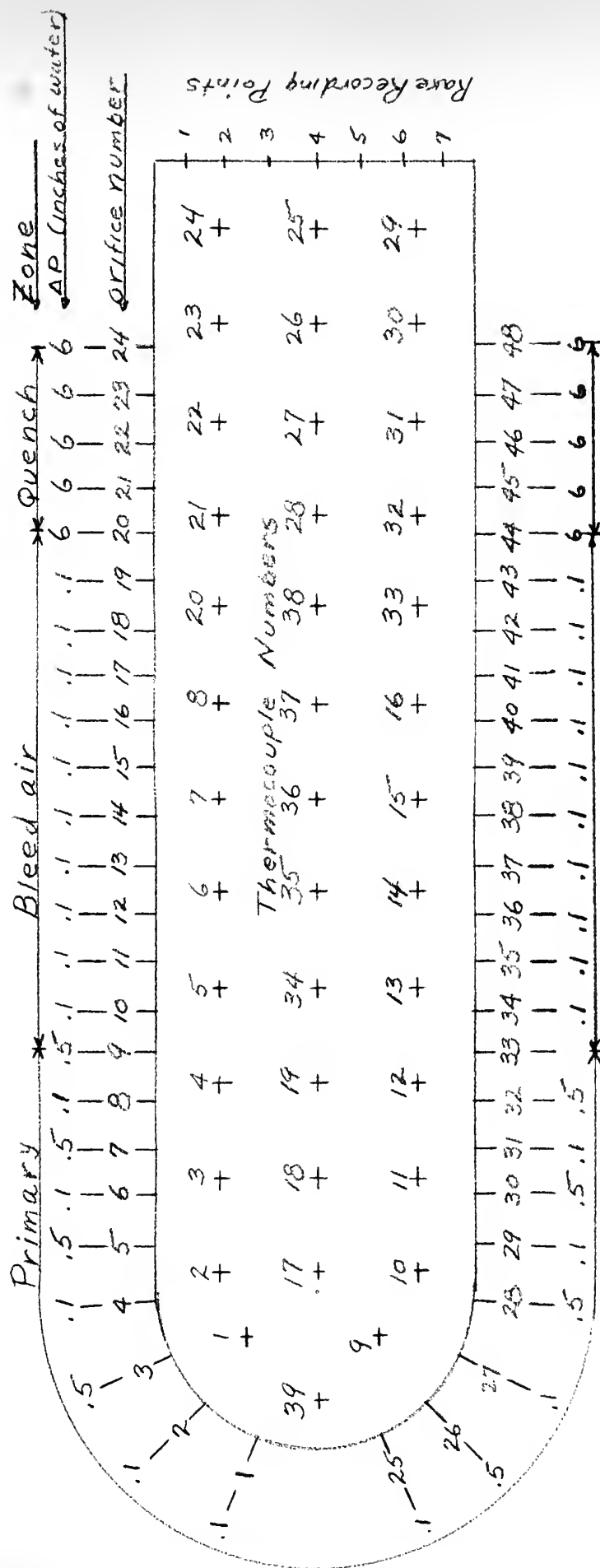


FIGURE 13 - THERMOCOUPLE CONVERSION CURVE.



Typical Air Flow Pattern

Scale: 1" = 2.5"

Z-Position ~ 20

FIG. 14



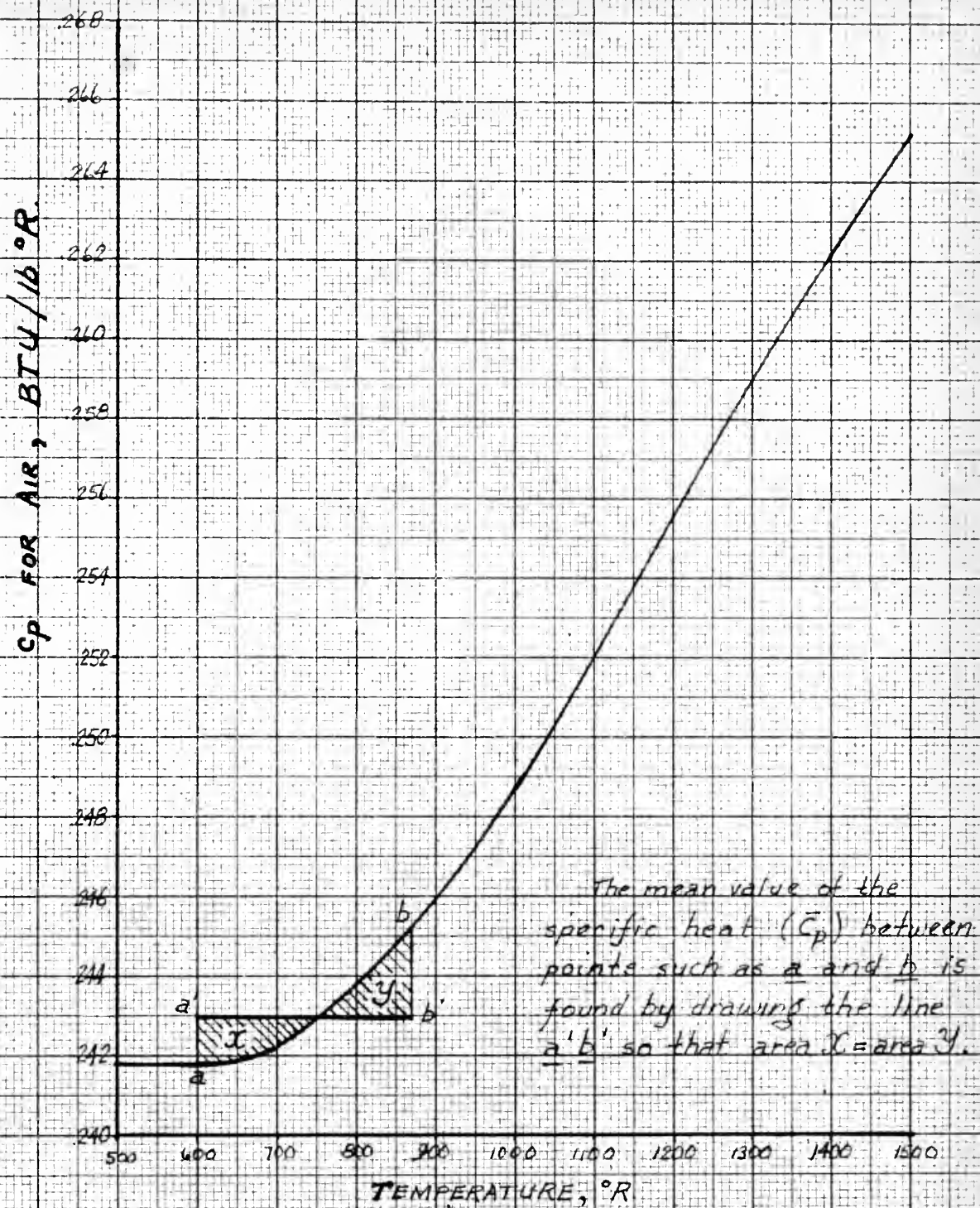


FIGURE 15 - DETERMINATION OF \bar{C}_p

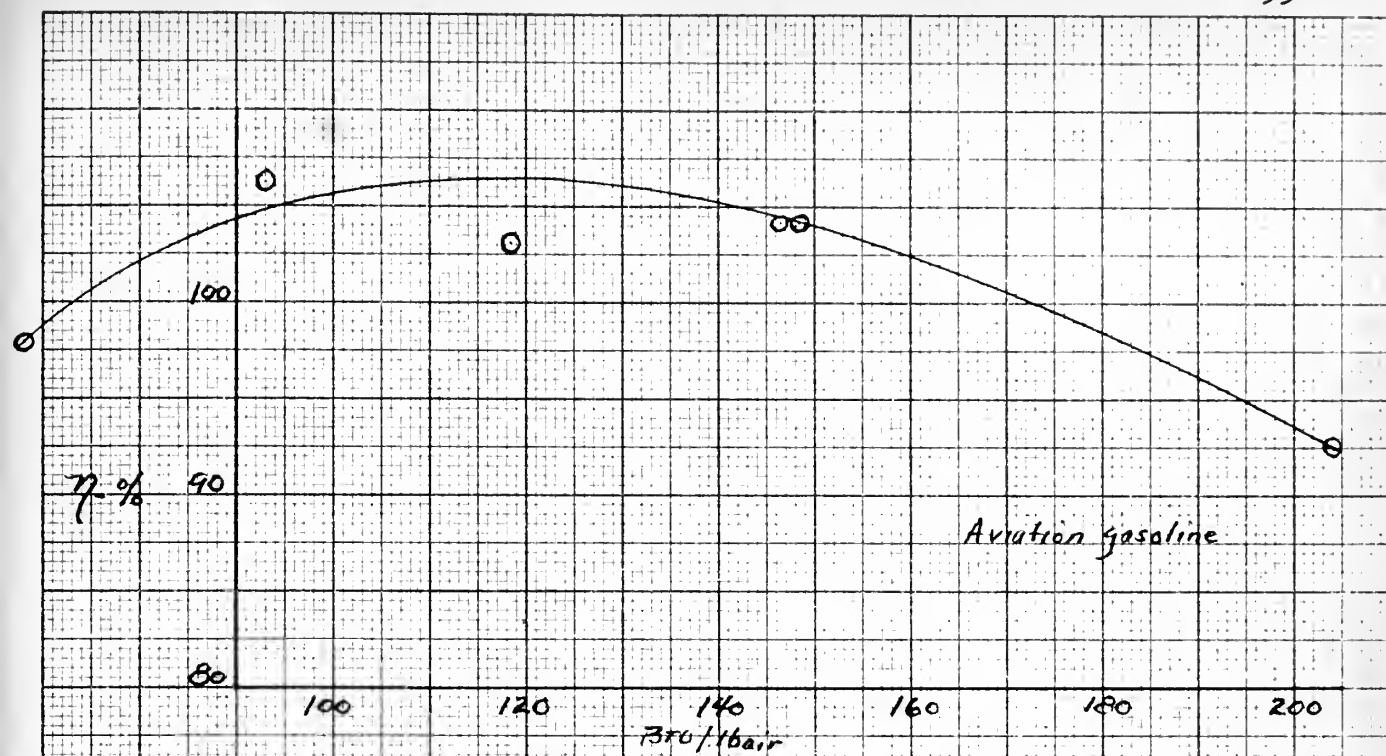


Fig. 16 - Efficiency vs Btu/lb air

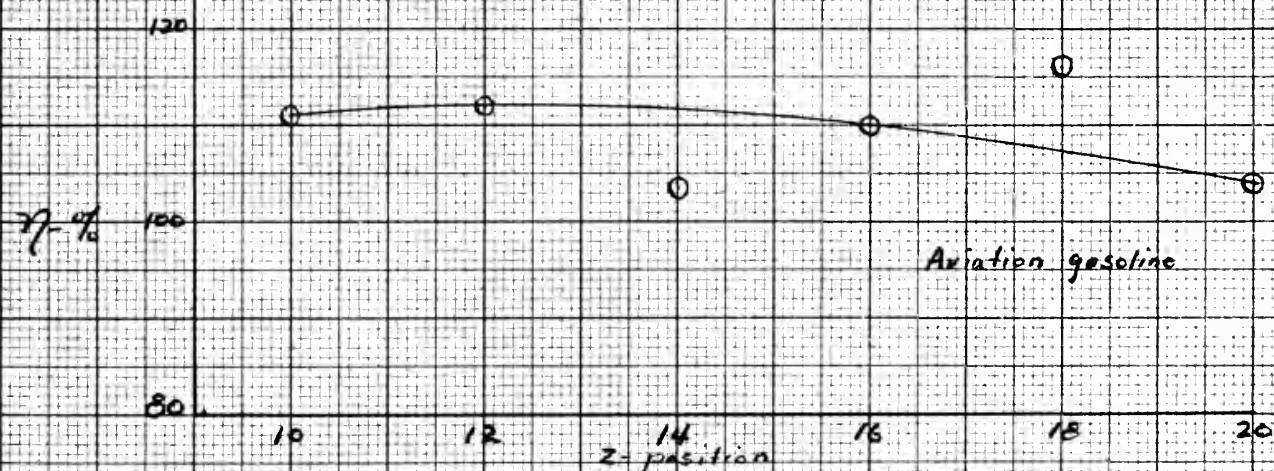


Fig. 17 - η vs Combustor Length (z-position)

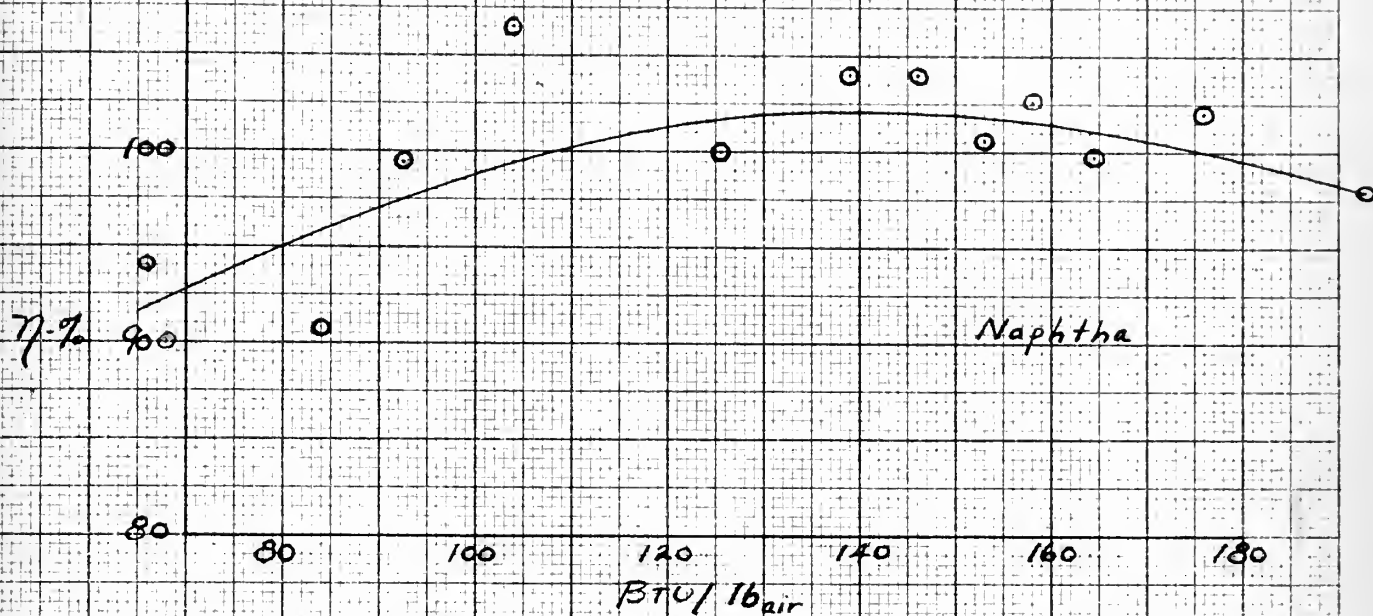


Fig. 18 - Efficiency vs BTU/lb_{air}

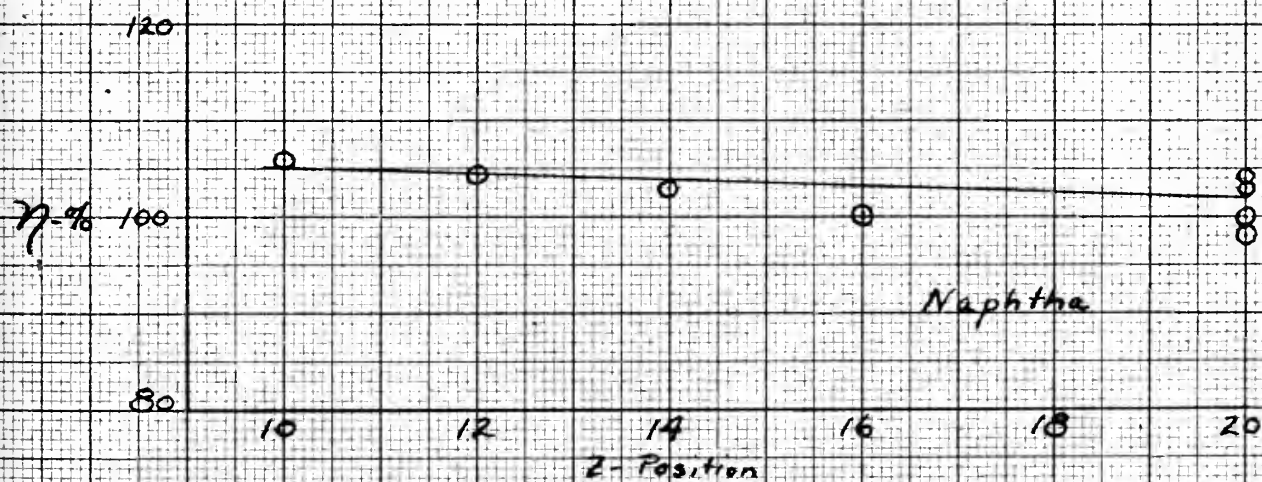
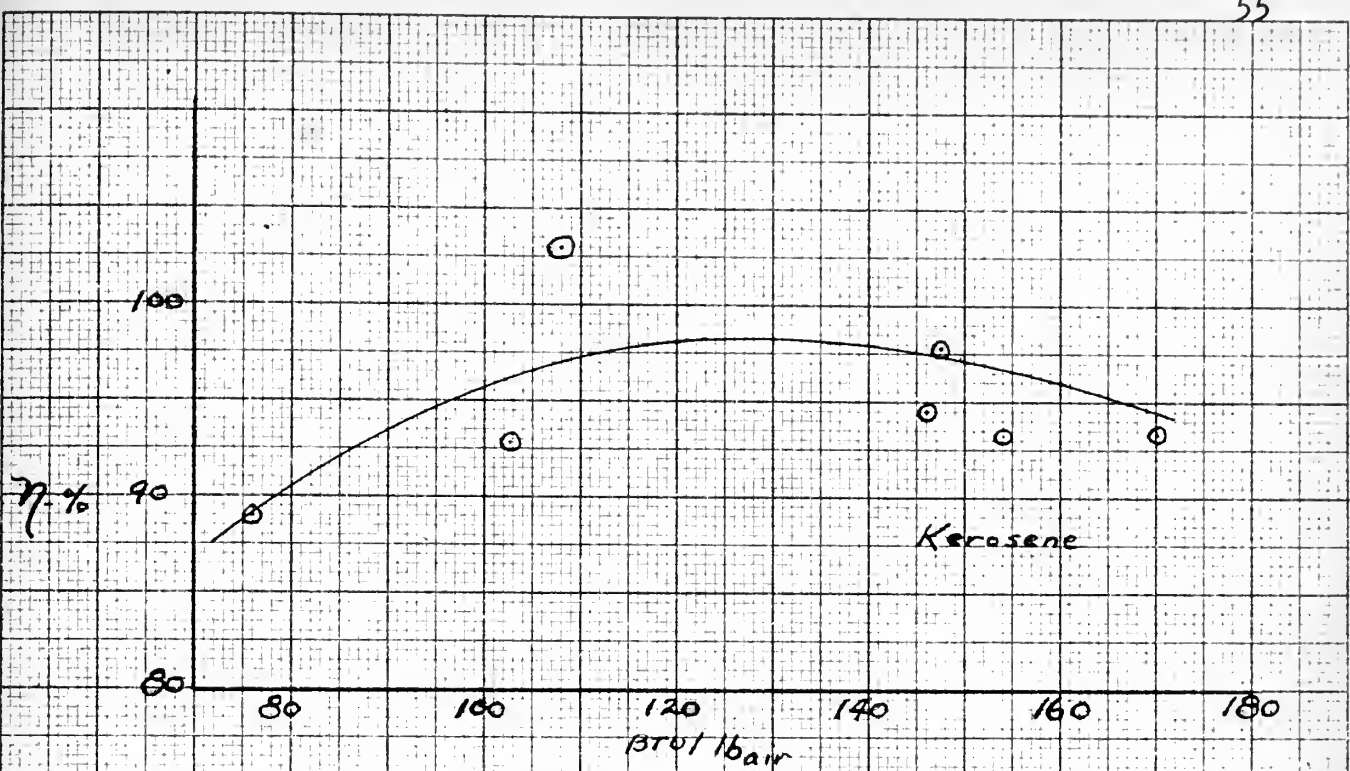
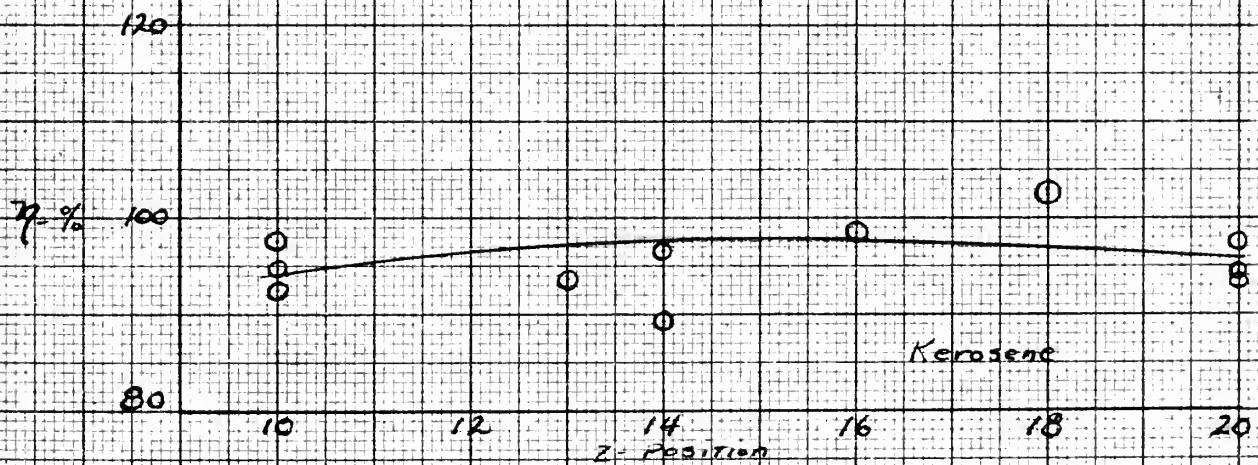


Fig. 19 - η vs Combustor Length (Z-position)

Fig. 20 - Efficiency vs. $Brul/bair$ Fig. 21 - η vs. Combustor Length (Z-position)

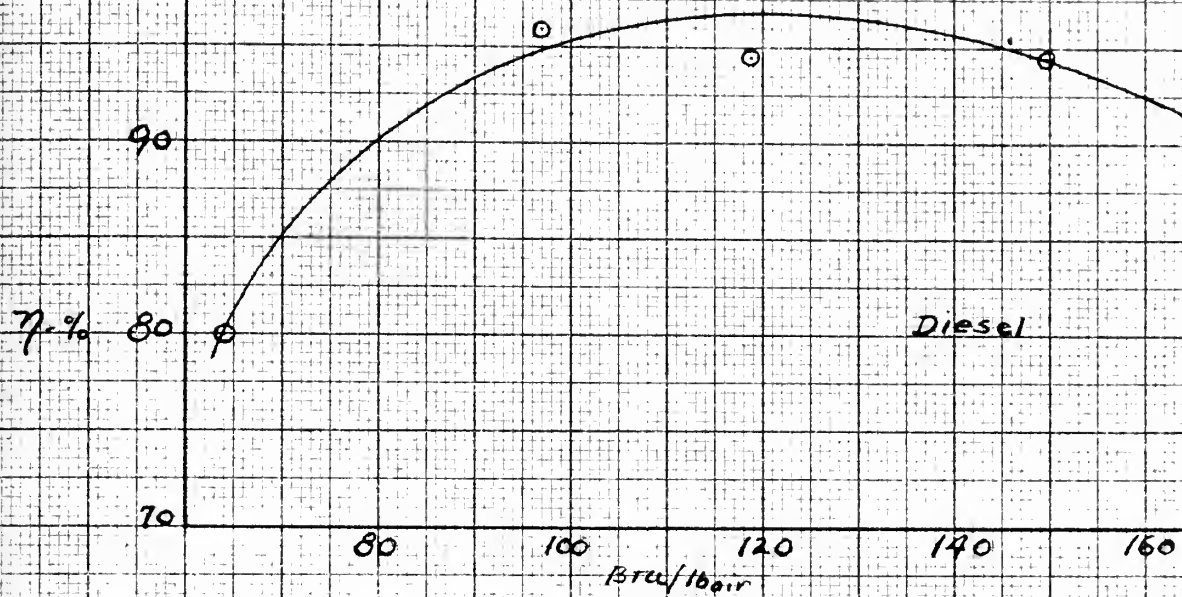
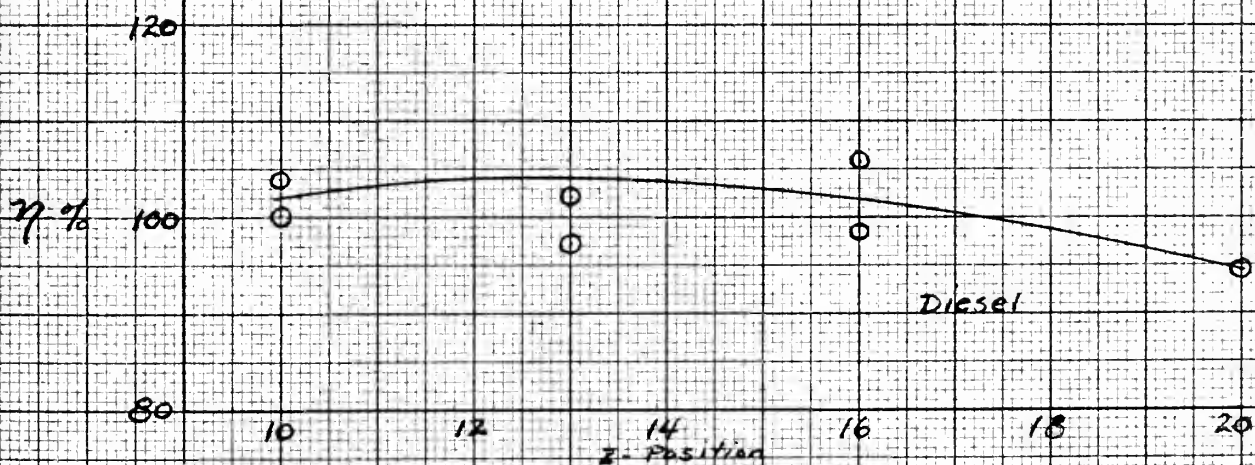


Fig. 22 - Efficiency vs. BTU/lb air

Fig. 23 - η vs. Combustor Length (Z-position)

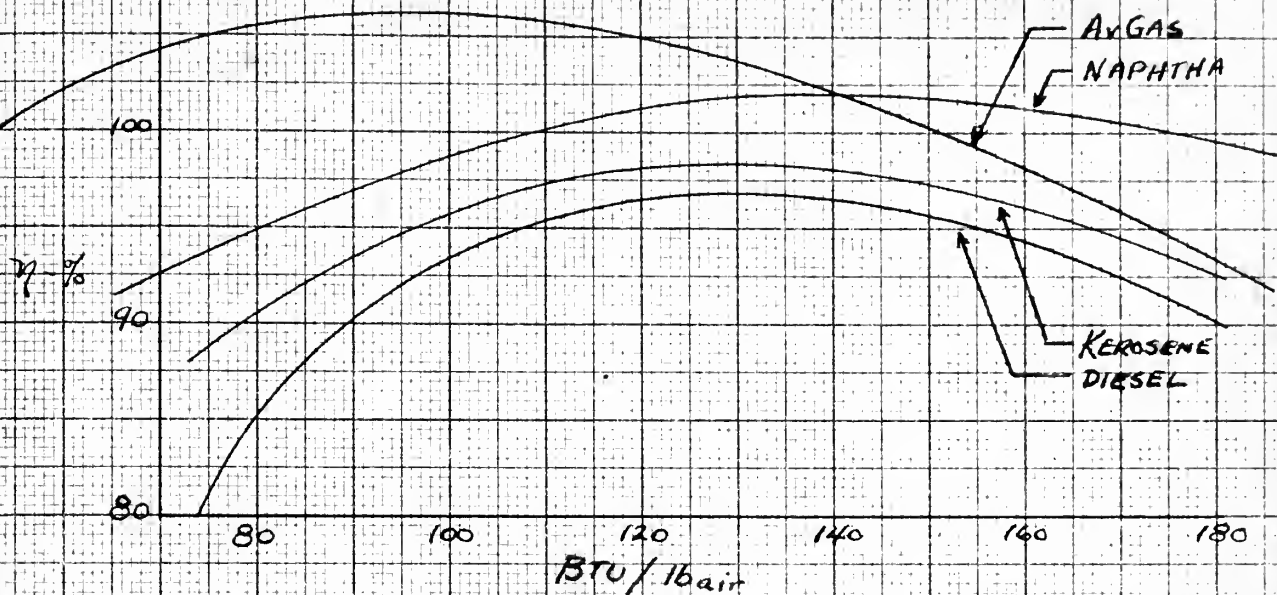


Fig. 24 - Efficiency vs BTU/lb air

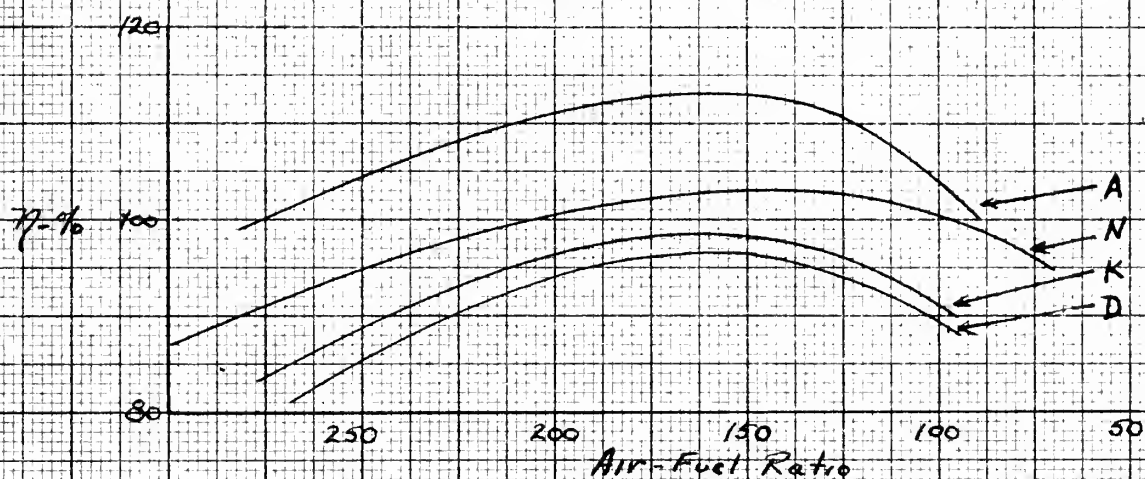


Fig. 25 - Efficiency vs Air-Fuel Ratio

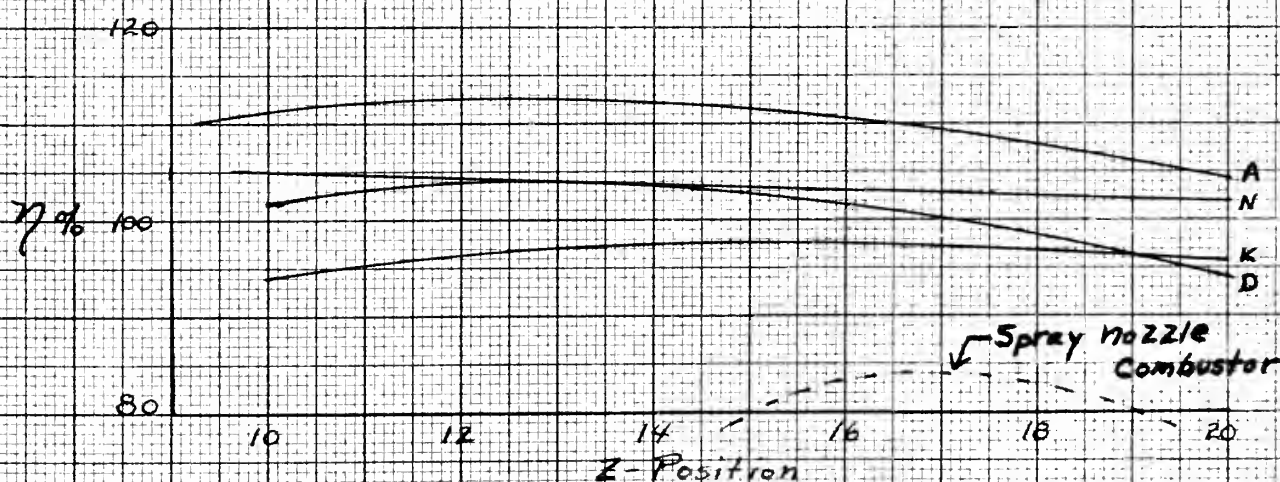
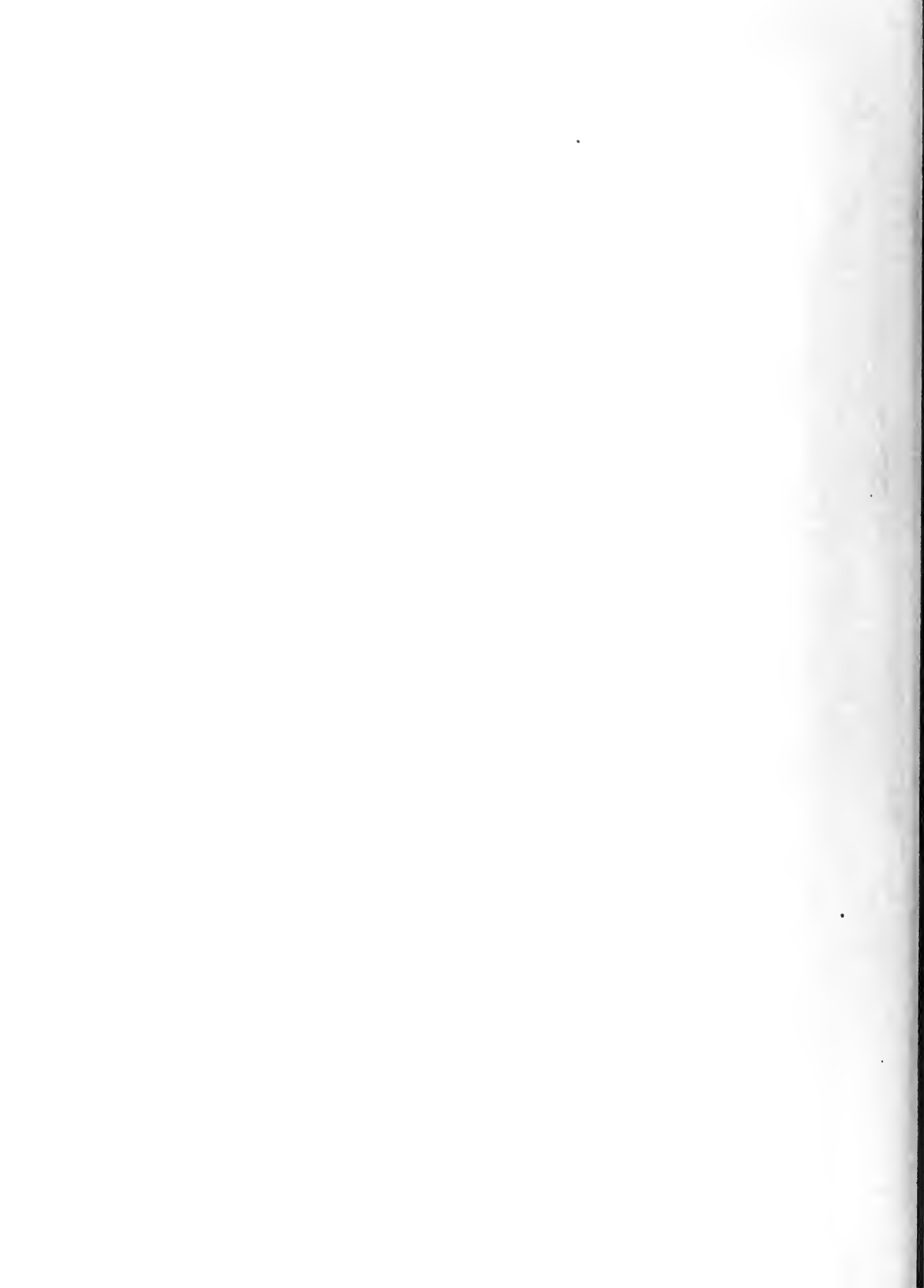


Fig. 26 - Efficiency vs Combustor Length (z-position)



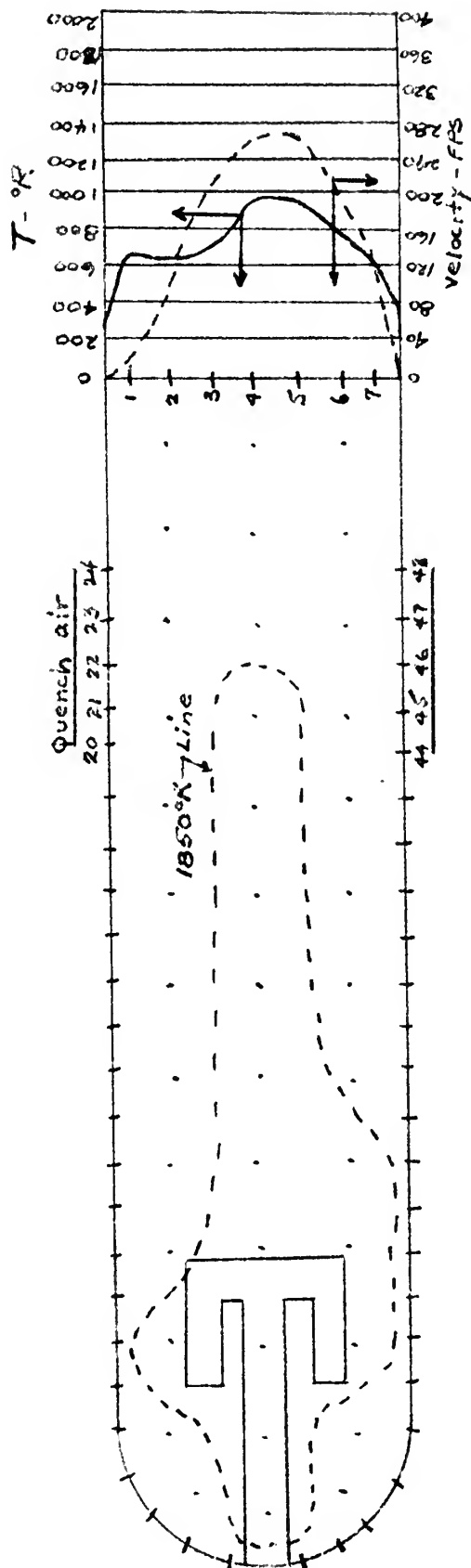
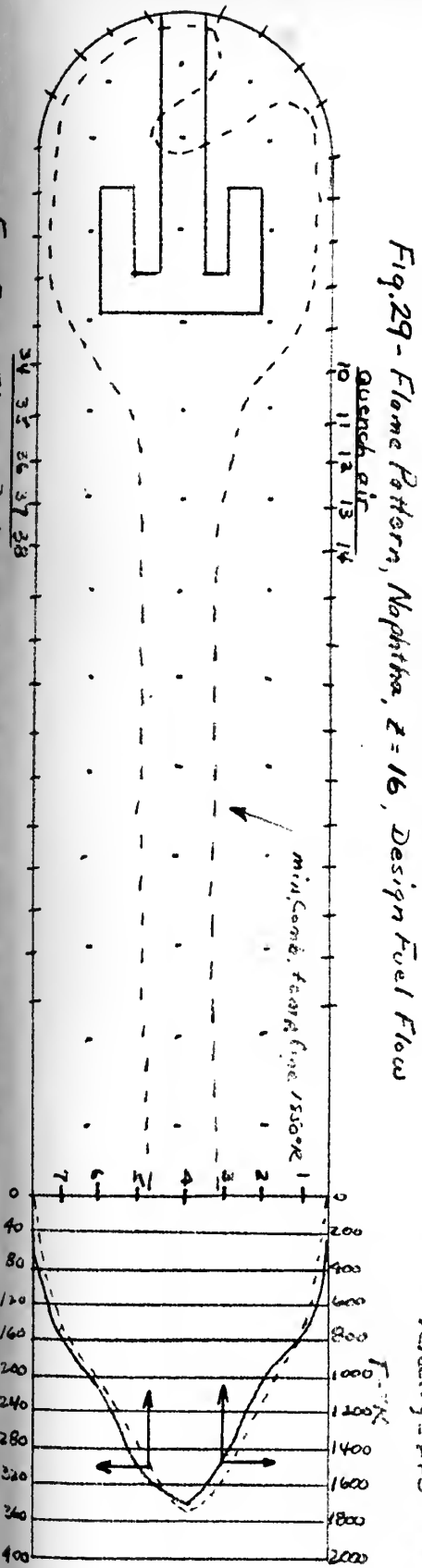
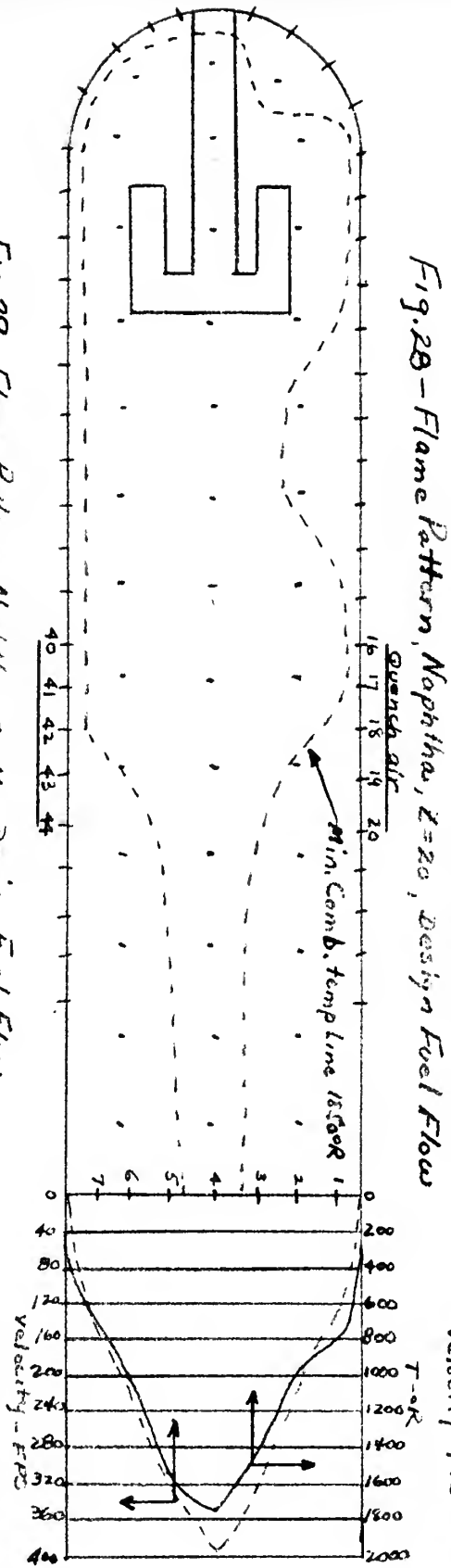
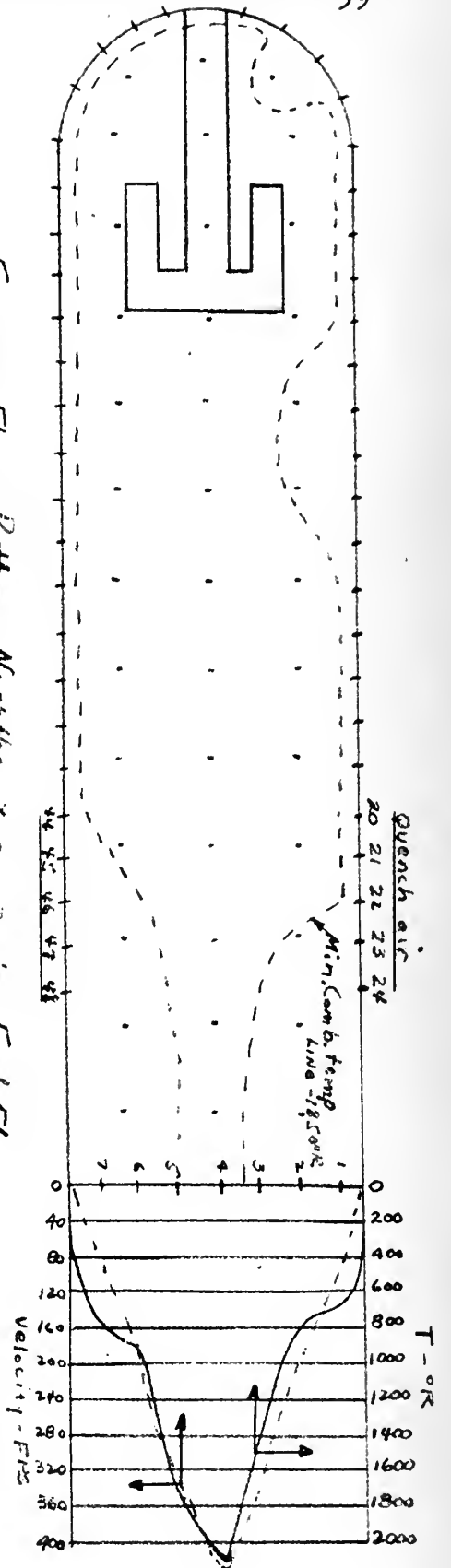


Fig. 27 - Flame Pattern, Naphtha, $Z = 20, 43.3\%$ Design Fuel Flow





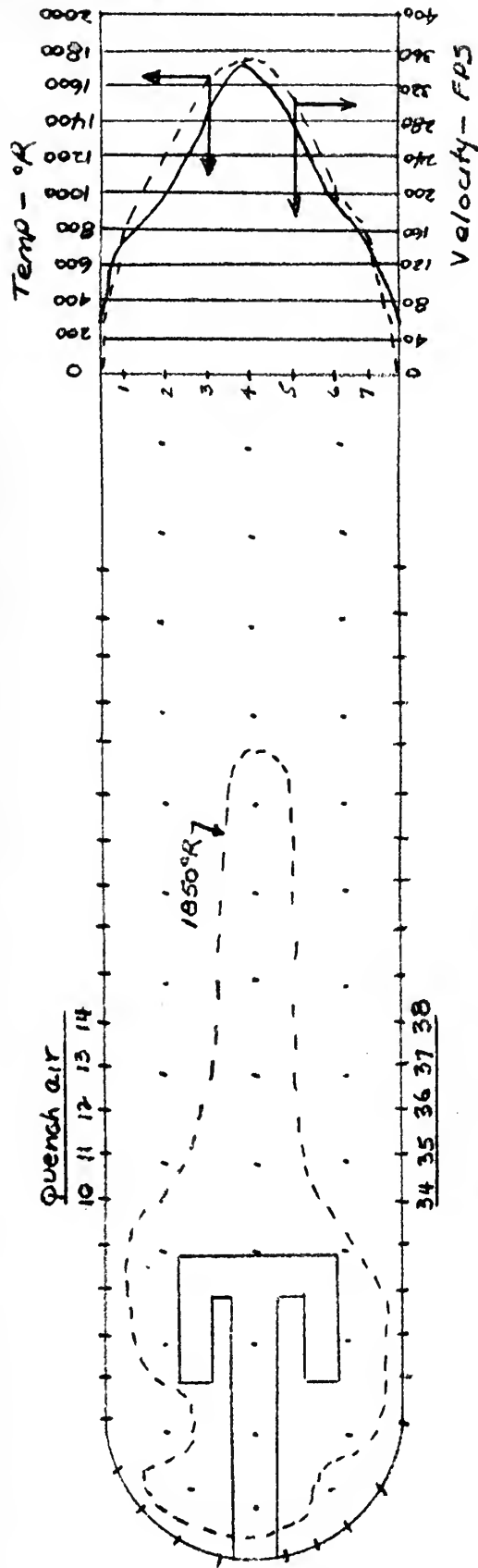


Fig. 31 - Flame Pattern, Diesel, z-position=10, Design Fuel Flow

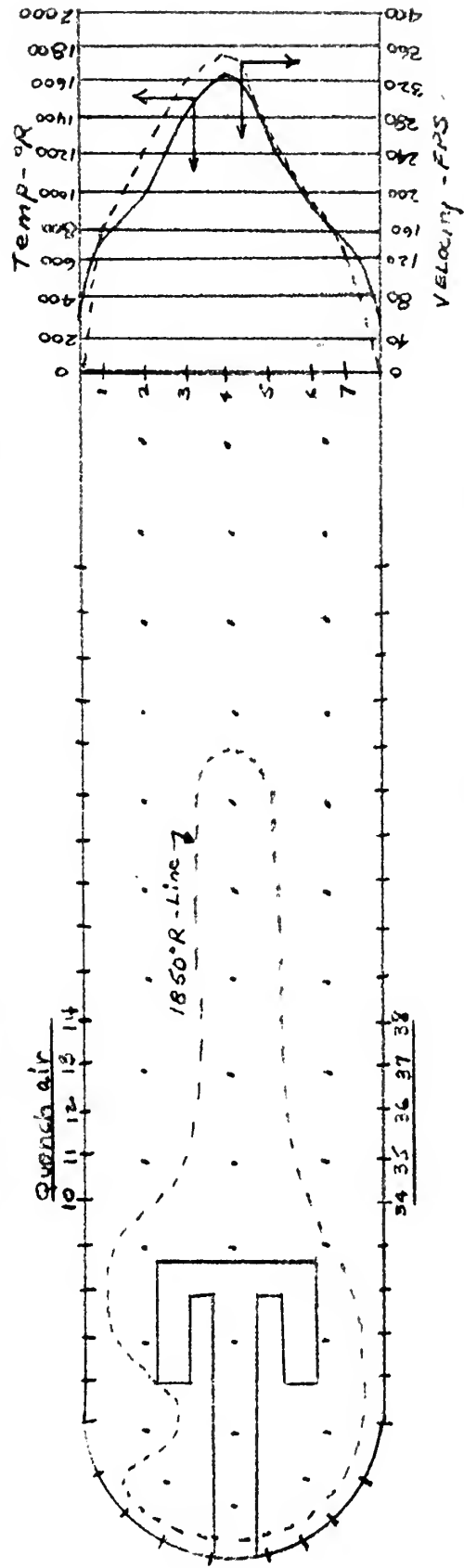


Fig. 32 - Flame Pattern, Kerosene, z-position=10, Design Fuel Flow



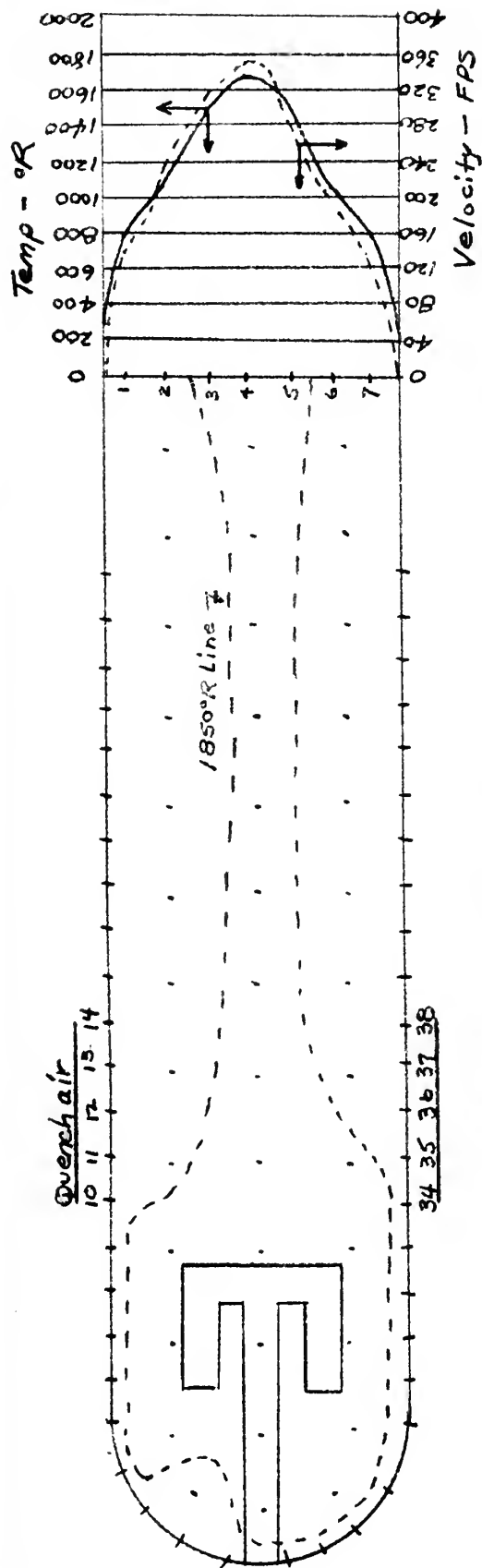


Fig. 33 - Flame Pattern - Aviation Gas, Z-position = 10, Design Fuel Flow

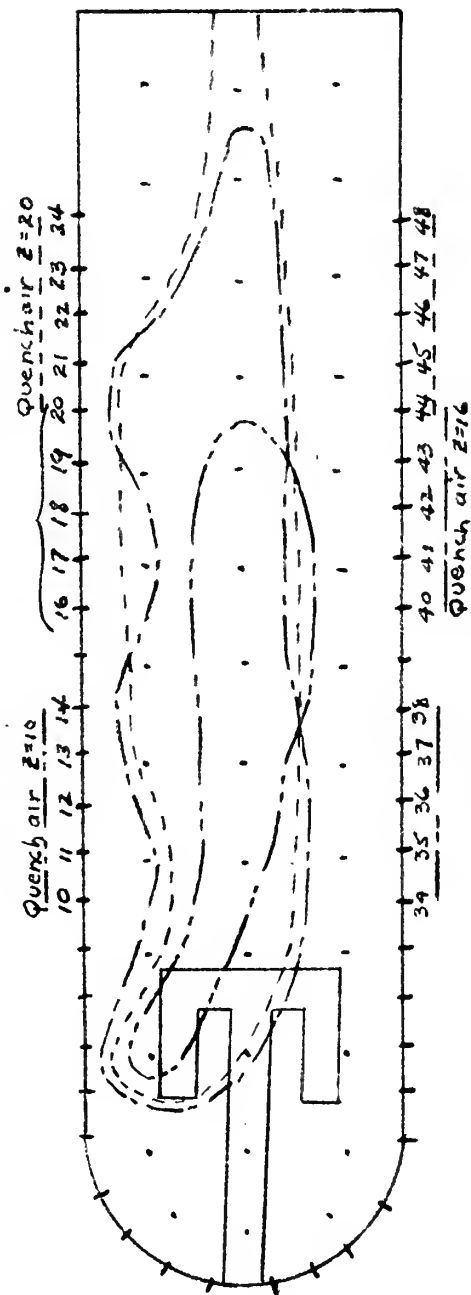


Fig. 34 - Flame Patterns, Kerosene; Z-positions 10, 16, 20; 75% Design Fuel Flow

--- Flame pattern for $Z=20$
 --- Flame pattern for $Z=16$
 --- Flame pattern for $Z=10$
 All outlines $\sim 1850^{\circ}\text{R}$



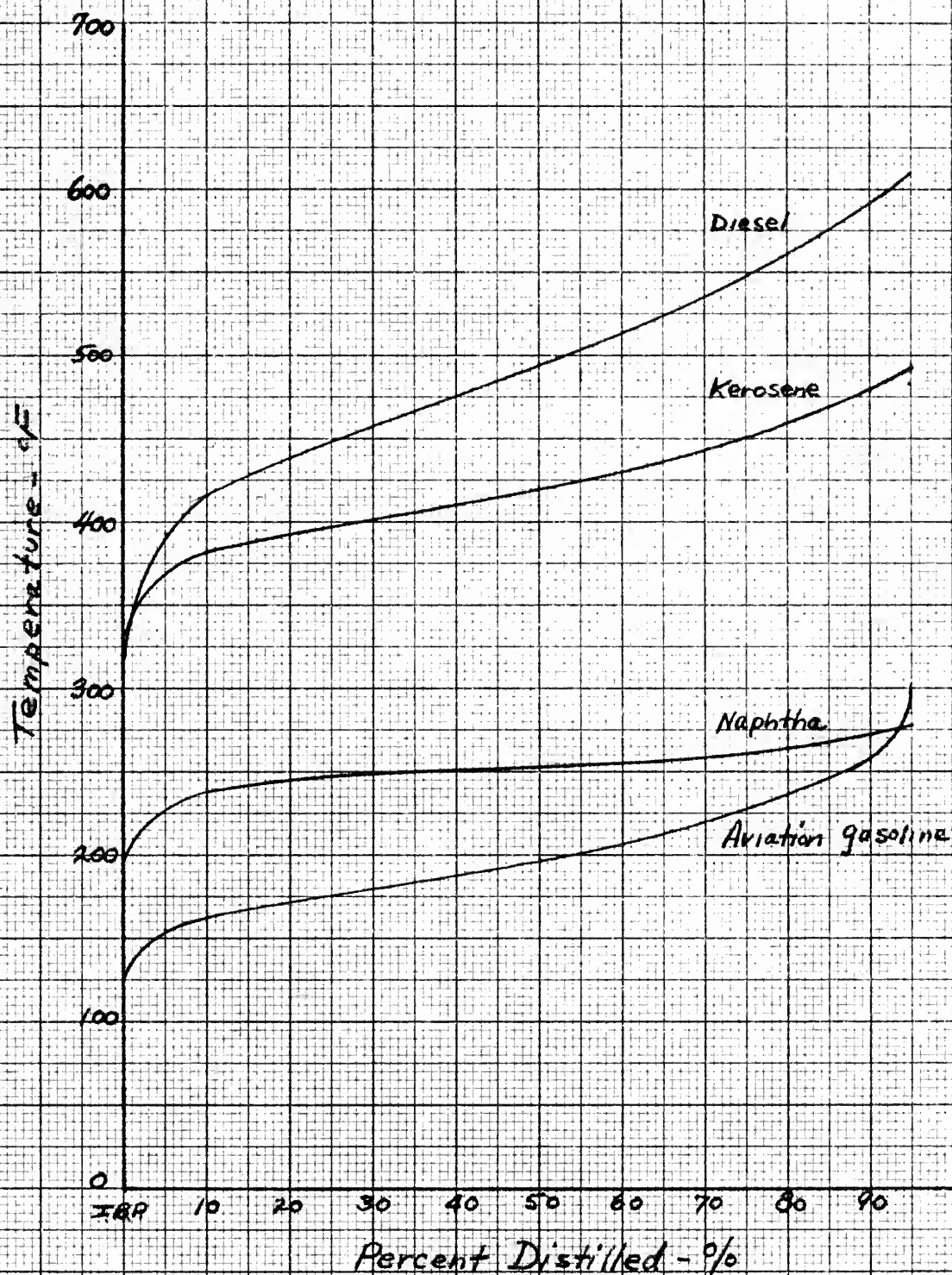


Fig. 35 - ASTM Fuel Distillation

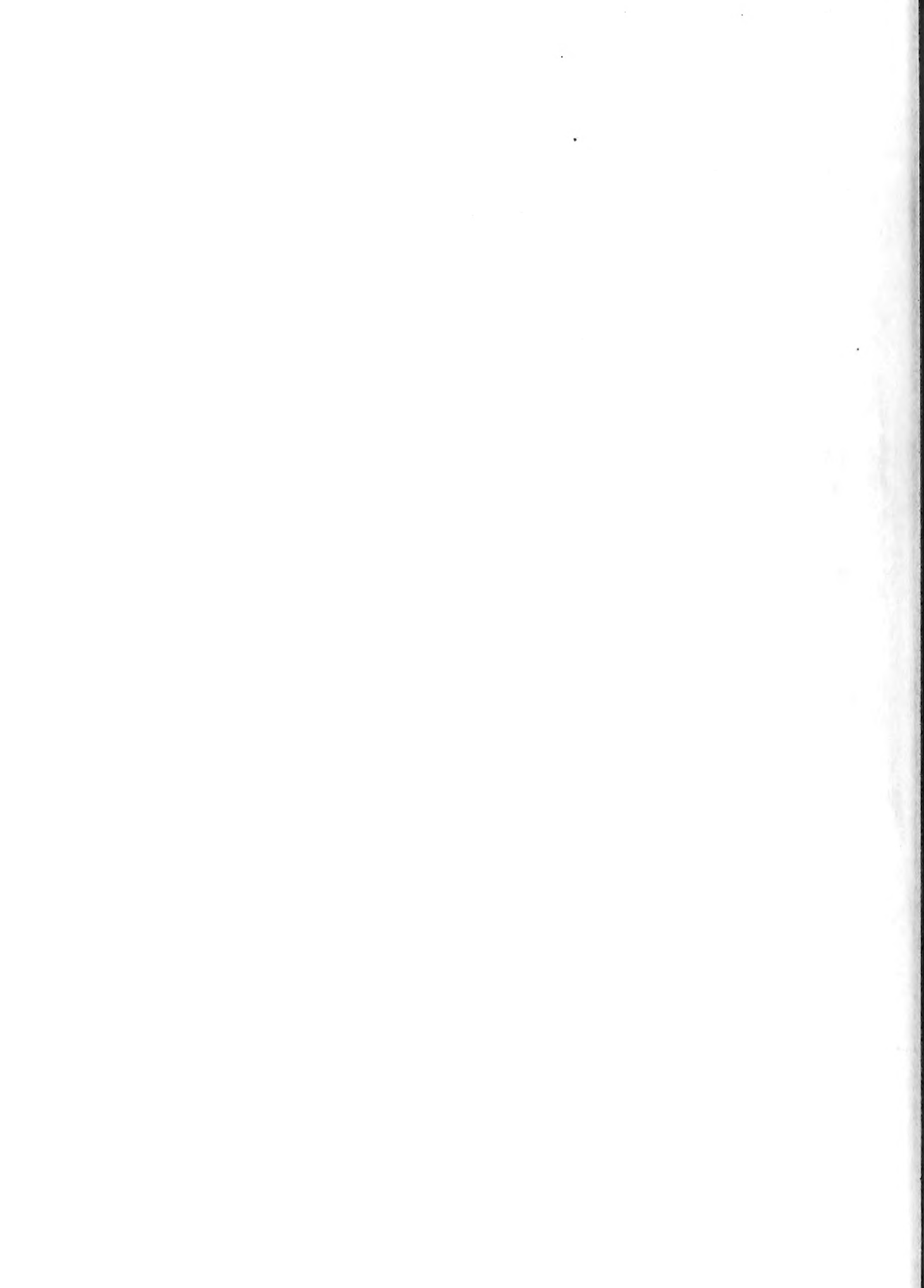


BIBLIOGRAPHY

1. Smith, G. Geoffrey. Gas Turbines and Jet Propulsion for Aircraft. New York: Aircraft Books Inc., 1946.
2. Griswold, John. Fuels, Combustion and Furnaces. New York: McGraw Hill Book Co., Inc., 1946.
3. Mock, F.C. "Engineering Development of the Jet Engine and Gas Turbine Burner," SAE Transactions, Vol. 54, 1946, pp. 218-227.
4. Jost, Wilhelm. Explosion and Combustion Processes in Gases. New York: McGraw Hill Book Co., Inc., 1946, Chapt. XI.
5. Olsen, L.A., Ruegg, F.W., and Caldwell, F.R. "Combustion in Moving Air," SAE Quarterly Transactions (April 1949), pp. 327-340.
6. Dugger, G.L. "Effect of Initial Mixing Temperature on Flame Speeds and Blow-Off Limits of Propane-Air Flames," NACA TN 2170, Aug. 1950.
7. Miller, W.L. "Design and Performance of a Vaporizer Type Fuel Inlet System," An M.S. Thesis submitted to the University of Minnesota, 1954.
8. Pouchot, W.D. and Hamm, J.R. "Characteristics of a Vaporizer Combustor For Aviation Gas Turbines," Advanced Paper No. 53-A-182 to be presented at ASME meeting Nov. 29, 1953.
9. Seippel, Claude. "Gas Turbines in Our Century," Transactions ASME, Feb. 1953, Vol. 75, p. 231.
10. Janssen, J.E. "A Preliminary Investigation Into the Effect of Air Distribution on Mixing in a Constant Pressure Combustion Chamber," An M.S. Thesis submitted to the University of Minnesota, 1953.
11. Flow Measurements, 1949, ASME Power Test Codes.
12. Ryberg, J. "The Effect of Various Liquid Fuels on the Optimum Length of an Open Cycle Gas Turbine Burner," An M.S. Thesis submitted to the University of Minnesota, 1953.
13. North American Combustion Handbook, Cleveland, Ohio, The North American Manufacturing Co., 1952.
14. ASTM Test Code: D86-40.



15. ASTM Test Code: D323-43.
16. Hutches, R.S. "An Investigation of the Effects of Turbulent Quenching in a Can Type Combustion Chamber," An M.S. Thesis submitted to the University of Minnesota, 1954.
17. Olson, W.T. and Bernardo, E. "Temperature Measurements and Combustion Efficiency in Combustors for Gas Turbines," ASME Transactions, Vol. 70, 1948, p. 329.
18. Eshbach, O.W. Handbook of Engineering Fundamentals, New York: John Wiley and Sons, Inc., 1936.





OCT 7

DISPLAY

25004

Thesis Barnes

B23

A study of the effect of various fuels on the optimum length of a gas turbine combustor equipped with a vaporizer tube.

OCT 7

DISPLAY

25004

Thesis
B23

Barnes

A study of the effect of various fuels on the optimum length of a gas turbine combustor equipped with a vaporizer tube.

the:B23

A study of the effect of various fuels o



3 2768 002 01434 2

DUDLEY KNOX LIBRARY